Advantages of an innovative vertical breakwater with an overtopping wave energy converter

Article *in* Coastal Engineering · May 2020

DOI: 10.1016/j.coastaleng.2020.103713

CITATIONS
5

READS
441

6 authors, including:

Enrico Di Lauro
International Marine and Dredging Consultants (IMDC nv), Antwerp, Belgium
26 PUBLICATIONS **362** CITATIONS
SEE PROFILE

Maria Maza
IHCantabria, Universidad de Cantabria
42 PUBLICATIONS **944** CITATIONS
SEE PROFILE

Javier L. Lara
Universidad de Cantabria
156 PUBLICATIONS **4,024** CITATIONS
SEE PROFILE

Pasquale Contestabile
Università degli Studi della Campania "Luigi Vanvitelli
76 PUBLICATIONS **1,319** CITATIONS
SEE PROFILE

Coastal Engineering 159 (2020) 103713

Contents lists available at ScienceDirect

Coastal Engineering

journal homepage: http://www.elsevier.com/locate/coastaleng

Advantages of an innovative vertical breakwater with an overtopping wave energy converter

Enrico Di Lauro [a,*], Maria Maza [b], Javier L. Lara [b], Inigo J. Losada [b], Pasquale Contestabile [a], Diego Vicinanza [a,c]

[a] Dipartimento di Ingegneria, Università della Campania "Luigi Vanvitelli", Via Roma 29, 81031, Aversa, Italy
[b] IHCantabria - Instituto de Hidráulica Ambiental de la Universidad de Cantabria, C/Isabel Torres 15, Parque Científico y Tecnológico de Cantabria, 39011, Santander, Spain
[c] CNR-INM, Institute of Marine Engineering, Via di Vallerano 139, 00128 Roma, Italy

ARTICLE INFO

Keywords:
Innovative breakwater
Numerical analysis
Hydraulic performance
Stability analysis

ABSTRACT

This paper presents an innovative vertical breakwater cross-section integrating an overtopping wave energy converter, named OBREC-V, and the analysis of its hydraulic performance and stability response to hydraulic loading. The structure is composed of a vertically-faced caisson with a sloping ramp on the top, a reservoir and a set-back crown-wall. The analysis of the structure is carried out by performing numerical simulations based on the Volume-Averaged Reynolds Averaged Navier-Stokes (VARANS) equations. The numerical simulations are performed to compare the performance of a traditional and innovative vertical caissons under the action of irregular waves, in terms of wave reflection, overtopping and wave acting forces. Results show that the reflection coefficients are lower than those computed in front of the traditional breakwater, with a reduction of up to the 40%. New formulations are proposed to better estimate the reflection coefficient and the wave overtopping at the rear side of the structure taking into account the non-conventional geometry of the device. The analysis of the forces indicate that the non-conventional geometry of the innovative OBREC-caisson increases the overall stability of the structure. The values of the safety factor against sliding, C_s, on innovative caissons are similar or greater than those calculated on the traditional vertical structure for almost all the tests. The downward force on the ramp and reservoir and the time lag between the vertical and horizontal forces, lead to a significant reduction of the maximum destabilizing forces F_s in the innovative breakwater, whose values range between 60 and 80% of the ones computed on the traditional structure. The obtained results show the co-benefits, in terms of functionality and hydraulic stability, that an OBREC-V entails with respect to a traditional vertical breakwater.

1. Introduction

Engineers and researchers working on coastal structures design have proposed a solution to significantly decrease the Wave Energy Converters (WECs) costs, which are still very high (Uihlein and Magagna, 2016). The idea consists of the development of devices that can be totally integrated into existing or expanding coastal infrastructures (Vicinanza et al., 2019; Rosa-Santos et al., 2019). These innovative hybrid structures still have their main function of sheltering a location from the action of waves, but with important benefits of the energy production due to the inclusion of a WEC. Inspired by the extensive investigation carried out on the Slot-Cone Generator, SSG (Vicinanza et al., 2012), a device denominated Overtopping BReakwater for Energy Conversion (OBREC) is currently under development. The OBREC is an innovative harbour defence structure with a special shape designed to accommodate an OverTopping Device (OTD). It consists of a concrete structure with a frontal ramp and, contrary to the SSG, only one reservoir, whose base is located above the water level. This technology is able to capture and collect part of the energy from incident waves that overtop the frontal sloping ramp. The potential energy of the water stored in the reservoir is then converted into kinetic energy, exploiting the hydraulic head between the reservoir and the sea water level. The water flows through low-head hydraulic turbines, located in a machine room behind a vertical crown-wall, for the energy conversion. The

* Corresponding author.
E-mail addresses: enrico.dilauro@hotmail.it (E. Di Lauro), mariaemilia.maza@unican.es (M. Maza), jav.lopez@unican.es (J.L. Lara), inigo.losada@unican.es (I.J. Losada), pasquale.contestabile@unicampania.it (P. Contestabile), diego.vicinanza@unicampania.it (D. Vicinanza).

https://doi.org/10.1016/j.coastaleng.2020.103713
Received 8 November 2019; Received in revised form 7 April 2020; Accepted 18 April 2020
Available online 10 May 2020

integration of an OBREC into a rubble-mound breakwater has been investigated over the last years with physical (Vicinanza et al., 2014; Contestabile et al., 2017b) and numerical model tests (Di Lauro et al., 2019; Palma et al., 2019), and it is still under development with the ongoing monitoring activities at full-scale in real environments (Contestabile et al., 2017a, 2019). The relatively simple geometry of this OTD-device, with a single frontal ramp and a reservoir, makes the technology suitable to be fully integrated also into vertical breakwaters.

The growing demand of seaward port expansion in relatively deep waters has promoted the development of this structural typology of harbour protection, making vertical breakwaters a better alternative in terms of performance and costs, when compared to traditional rubble mound breakwaters in many cases. Many innovations have been presented over the last decades to overcome the limits of traditional vertically-faced breakwaters. One of the greatest disadvantages of these harbour defence structures is the high reflection pattern in front of them and their exposure to large impulsive wave forces. If the reflection and the impact pressure are relevant issues, several structural measures can be taken, such as the use of top-sloping caissons, perforated Jarlan-type breakwaters, largely adopted in Japan (Takahashi, 2002) or breakwaters with a frontal basin '*Stilling Wave Basin*' (SWB) (Burcharth and Andersen, 2007; Geeraerts et al., 2007; Cappietti and Aminti, 2012; Van Doorslaer et al., 2015; Kisacik et al., 2019). Despite the different performance of these non-conventional configurations, all the typologies share the same goal, which is to protect the harbour by dissipating a larger amount of wave energy when compared to that dissipated by traditional caissons (Vicinanza et al., 2019).

Based on previous studies, such as the development of the OBREC integrated into a rubble-mound breakwater (Vicinanza et al., 2014), the SSG-integrated into a vertical breakwater (Vicinanza et al., 2012), and the concept of the vertical caisson with the SWB system, a novel caisson is proposed. This novel design consists of the integration of the OBREC device into a vertical structure. The structure, hereinafter referred to as OBREC-V, is composed of a vertically-faced caisson with a sloping ramp, a reservoir and a set-back crown-wall located on the top. At the rear side of the crown-wall, a machinery room is built to accommodate the instrumental apparatus for the energy conversion (i.e. low-head turbines and generators). A sketch of the OBREC-V is shown in Fig. 1. As in the case of traditional port breakwaters, the principal function of this caisson is the defence and protection of the inner area of the harbours. However, instead of completely reflecting the energy from the waves, it is designed to absorb part of the energy and convert it into electricity. This concept design adds a revenue wave generation function to a breakwater, adding benefits due to WEC integration (sharing-cost). This technology can be applied for new breakwaters of port expansions or integrated into existing ones, which have to be rebuilt due to maintenance activities, or upgraded due to climate change. As for the case of rubble-mound breakwaters (Vicinanza et al., 2014), the costs of the OBREC installation into new vertical breakwaters are lower compared to stand-alone WEC devices, considering that the caisson would be built regardless of the inclusion of the WEC, and geometrical changes affect only the superstructure.

One of the primary goals for coastal engineers involved in the development of a new WEC-integrated caisson concept, is assessing the breakwater hydraulic performance, compared to that of traditional breakwaters. Therefore, the main objective of this study is to evaluate processes such as wave reflection, overtopping over the crest and wave loading as a first step towards the analysis of the stability of the new concept. Please note that at this stage the evaluation of the WEC performance is out of the scope of this work.

The innovative characteristics of the cross section does not allow a direct application of conventional formulas for breakwater functionality or stability. Consequently, the evaluation requires the use of physical modelling or advanced numerical models. The results presented in this paper were obtained using of the numerical model IH2VOF, which has been extensively applied for wave-structure analysis with very accurate results in the prediction of the hydraulic response of vertical caissons (Lara et al., 2008; Losada et al., 2008; Guanche et al., 2009). Furthermore, IH2VOF has been thoroughly validated against physical model tests for an OBREC located on a rubble mound breakwater as shown in Di Lauro et al. (2019), providing further evidence that it is an excellent tool for assessing the performance of the new vertical caisson.

The present paper is organized as follows. The numerical model set-up is presented in Section 2 with a description of the numerical domain, the grid size dimensions, the generated wave characteristics as well as the different OBREC superstructure tested. Section 3 is devoted to the numerical results of the overtopping discharge and reflection coefficients, with a comparison between traditional and innovative caissons. A dimensional analysis is also presented, with the evaluation of the influence of the principal geometrical parameters on the overall hydraulic performance. The analysis of the wave forces exerted on the different configurations is presented in Section 4. Finally, conclusions are drawn in Section 5.

2. Numerical model set-up

At this early stage of development, the aim of the numerical analysis is to provide a preliminary optimization of the innovative caisson by evaluating the parameters that might have an influence on its hydraulic performance. In order to provide a full comparison, the performance of the OBREC-V is tested against the one for a traditional vertical breakwater having the same overall dimensions (Fig. 2). Both structures are

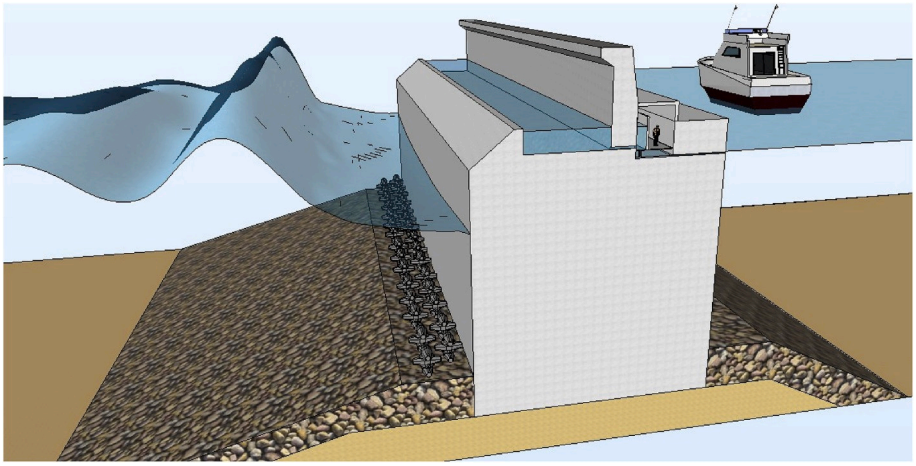

Fig. 1. Concept design of the innovative caisson integrated with an OBREC device.

located on an identical mound-foundation. The only difference between the two caissons is the superstructure, which consists of a conventional crown-wall for the traditional caisson and an OBREC device with a ramp, a reservoir and a set-back wall for the innovative structure. The numerical tests are carried out at 1:30 length scale (Froude scaling) compared to the prototype. The considered crest freeboard, R_c, is equal to 0.233 m and the caisson width, $B_{caisson}$, is equal to 0.667 m. The geometry of the traditional and innovative caissons is displayed in Fig. 2. The reason why the numerical simulations are performed at small scale is that IH2VOF has been already validated at a similar scale (Di Lauro et al., 2019) by comparing the numerical results with those measured at small-scale laboratory tests carried out at Aalborg University (Contestabile et al., 2017b). Using a pre-validated model strongly limits the introduction of additional uncertainties in the analysis.

The OBREC-V is characterized by the following geometrical parameters: the crest freeboard of the ramp, R_r, and the horizontal distance between the seaward caisson face and the set-back crown-wall, B_{wall}. These two parameters have been considered as the leading ones in the design of the device, as they are for the OBREC integrated in the rubble-mound breakwater, hereinafter referred to as OBREC-R (Iuppa et al.,

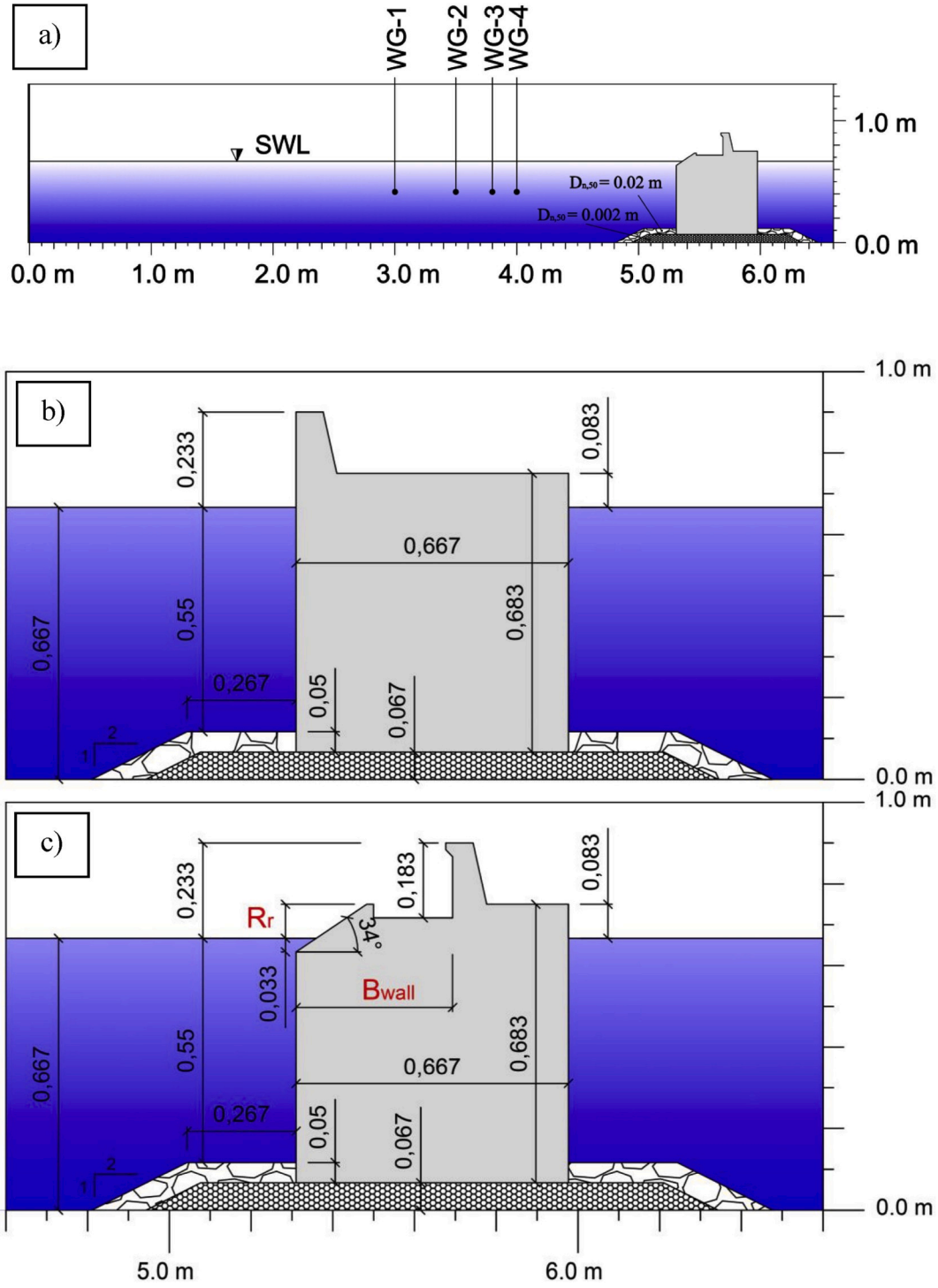

Fig. 2. Layout of the two-dimensional numerical domain, with the location of the innovative caisson and the numerical wave gauges (WG) on the upper panel (a); cross-section of the traditional caisson (b) and the innovative caisson integrated with the OBREC device (c).

2016; Contestabile et al., 2017b). Hence, their influence on the hydraulic and structural response of the novel caisson is investigated here. As shown in Fig. 2, the ramp has a slope of 34° with respect to the horizontal. The slope has been selected considering the same values of the flat ramp slope of the OBREC-R. That slope was chosen to minimize the occurrence of breaking waves and to maximize the wave overtopping into the reservoir, considering it as optimal (Contestabile et al., 2017b). Three values of R_r, and as many of B_{wall}, are considered, for a total of nine different geometrical configurations (see Fig. 3). These configurations were tested using an identical numerical domain with a total length of 6.6 m and a height of 1.30 m, as displayed in the top panel of Fig. 2. The material properties of the porous layers are set according to the numerical test set-up described by Di Lauro et al. (2019), which has been thoroughly validated against the laboratory tests described in Contestabile et al. (2017b). In detail, the porous media below each caisson base is composed of an internal layer with a nominal diameter $D_{n,50} = 5$ mm and porosity $n = 0.40$, and seaward and leeward external armour layers with $D_{n,50} = 20$ mm and $n = 0.45$. Furthermore, the value of the empirical coefficient, α, in the VARANS equations (Losada et al., 2016) is set to 200 for all the porous layer, while the empirical coefficient, β, is set to 0.8 for the internal layer and 1.0 for the external layers, according to Lara et al. (2008), Losada et al. (2008) and Guanche et al. (2009). The added mass coefficient, c, is set to a constant value equal to 0.34 for all porous media, according to the suggestion of van Gent (1995).

The base reservoir is modelled in IH2VOF as a closed structure, similar to the OBREC-R described by Di Lauro et al. (2019). Only extreme wave conditions are generated for this analysis, hence the OBREC model's reservoir is saturated during the whole duration of the numerical tests. Considering that R_r/H_{m0} ranges between 0.200 and 0.643 and based on the results of the overtopping into the OBREC reservoir obtained by Iuppa et al. (2016), the assumption of a closed reservoir as modelled with IH2VOF in this paper is considered to be valid.

In order to properly reproduce the wave generation and reflection pattern, the seaward vertical face of the caisson is located in the numerical domain at a distance of 5.31 m from the wave maker (inlet boundary layer), corresponding to 1.2–1.5 times the deep water wave length, $L_{-1,0}$, based on the energy period $T_{m-1,0}$. The first wave gauge ($WG-1$) is placed at 3 m from the inlet and the other three free surface gauges at 0.50 m, 0.80 m and 1.00 m from the position of $WG-1$. The numerical incident and reflected spectra are separated and estimated using the Zelt and Skjelbreia (1993) method. First order irregular wave time series are generated in IH2VOF as a linear superposition of Stokes I waves for a given number of components ($N = 512$). A standard JONSWAP-type spectrum (Hasselmann et al., 1973), with a peak enhancement factor of 3.3, is considered for all the tests. Active wave absorption is considered in the inlet boundary following a procedure similar to the one used in physical wave flumes and proposed by Schaffer and Klopman (2000). Details of the implementation of the active absorption in IH2VOF are described in Lara et al. (2011). An open boundary with a wave absorption condition is considered at the outlet boundary layer, following the methodology proposed by Schaffer and Klopman (2000).

In order to analyse the structure, nine wave conditions are simulated in the numerical flume. Table 1 summarises the wave parameters of the waves generated in the numerical domain, while Table 2 shows the nondimensional parameter ranges tested in the analysis. Characteristics of the generated waves have been chosen to cover a wide range of extreme wave conditions, with low values of R_r/H_{m0}, for the assumption of the saturated reservoir, and low values of R_c/H_{m0}, ensuring overtopping conditions for the traditional structure. Please note that R_c/H_{m0} ranges from 1.0 to 1.5, which are the typical design conditions for traditional vertical breakwaters in Europe (Franco, 1992).

Each wave-generated signal is adopted for all the geometrical

Table 1
Incident wave characteristics for numerical tests.

	H_{m0} (m)	T_p (s)	$T_{m-1,0}$ (s)	$T_{m,01}$ (s)	$T_{m,02}$ (s)
Test_01	0.157	1.452	1.296	1.218	1.169
Test_02	0.156	1.552	1.461	1.370	1.312
Test_03	0.156	1.845	1.686	1.582	1.517
Test_04	0.193	1.484	1.380	1.294	1.240
Test_05	0.189	1.750	1.572	1.475	1.415
Test_06	0.190	1.896	1.775	1.666	1.596
Test_07	0.230	1.665	1.504	1.415	1.359
Test_08	0.230	1.845	1.712	1.607	1.541
Test_09	0.229	2.133	1.929	1.810	1.736

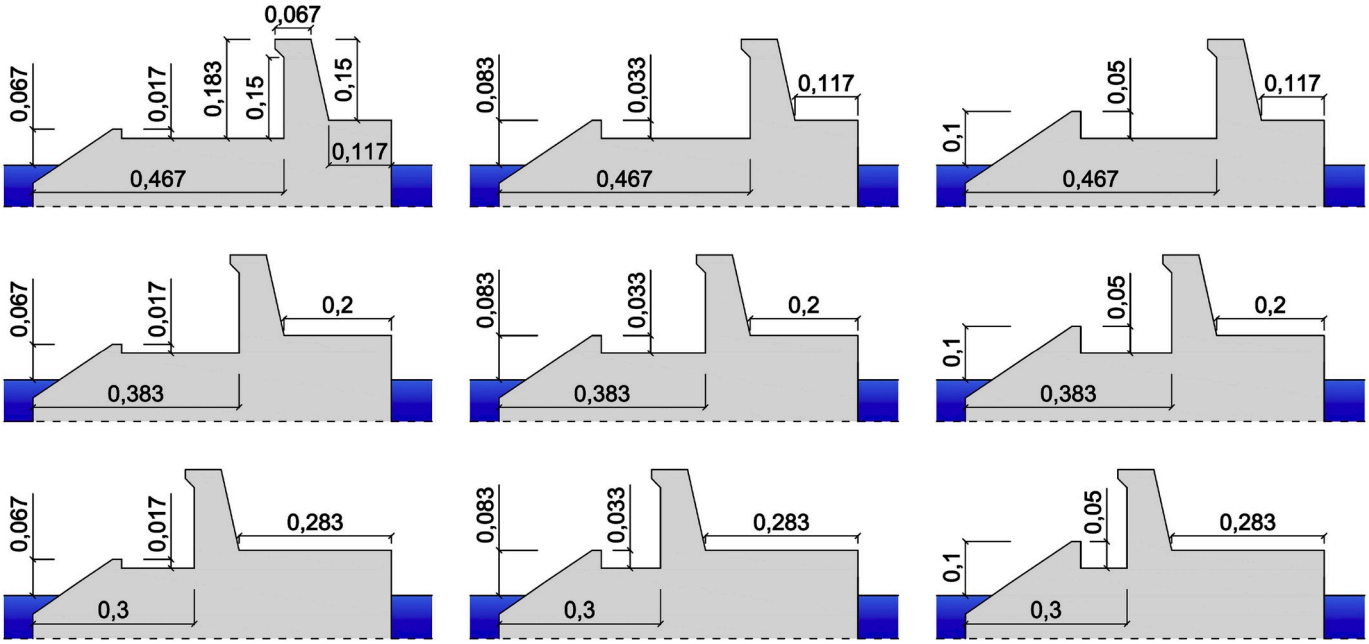

Fig. 3. Nine geometrical configurations of the OBREC-caisson tested with IH2VOF.

Table 2
Nondimensional parameter ranges for the numerical analysis.

	R_c/H_{m0} [−]	R_r/H_{m0} [−]	$B/L_{wall-1,0}$ [−]	H_{m0}/h [−]	$h/L_{-1,0}$ [−]	$H/L_{m0-1,0}$ [−]	h/H_{m0} [−]
Min	1.015	0.290	0.069	0.233	0.154	0.043	2.901
Max	1.501	0.643	0.190	0.345	0.272	0.074	4.287

configurations, for a total of 90 numerical tests (9 wave conditions x 10 geometrical configurations). The use of identical wave generation signals allows comparing wave-by-wave the different geometries tested in the numerical flume, evaluating in more detail the differences in terms of wave reflection, overtopping discharge and wave loading exerted on the structure. A constant water depth, h, of 0.667 m is considered for all the tests. Sea states of around 1000 waves are tested. Time series are chosen to be long enough to fully define reliable wave spectra. Moreover, the length of each test can be considered sufficient to obtain consistent statistical values of the peak pressures/forces, as well as to perform the necessary statistical reliability for the wave overtopping analysis.

A variable grid size is considered along x and y. Fine discretization, $\Delta x = \Delta y = 0.007$ m is considered around the OBREC. The mesh varies gradually to a maximum grid size of $\Delta x = 0.021$ m and $\Delta y = 0.015$ m. The use of the highly refined computational grid mesh around the area of interest of the OBREC model ensures the correct simulation of the non-conventional geometry of the device with the presence of a sloping ramp and a parapet on the top of the vertical set-back wall. Moreover, this fine grid resolution allows resolving the large velocity variation near the solid wall during wave impact. The resultant numerical domain has 539 cells in the x-direction and 153 cells in the y-direction, leading to a total of 82,467 computational cells.

3. Hydraulic performance

3.1. Wave reflection

The effect of the innovative OBREC-V cross section on wave reflection was also evaluated using the numerical model. Comparisons with a regular cross section are provided using both the numerical model and the empirical formulation suggested by Allsop et al. (1994). Reflection is assessed by calculating the reflection coefficient, K_r, evaluated in the numerical model by using the method proposed by Zelt and Skjelbreia (1993). Numerical results of reflection coefficients in front of the structures are presented as a function of the relative crest freeboard R_c/H_{m0} (Fig. 4). Blue diamond's indicate the reflection coefficients for the traditional caisson (Fig. 2b), while red symbols represent the K_r values for the different OBREC-V configurations (Fig. 3). A dashed black line in Fig. 4 indicates the empirical relation proposed by Allsop et al. (1994). Reflection coefficients for the traditional structure match very well Allsop et al. (1994) formulation, with a mean K_r equal to 0.92. These results are in agreement with $K_f = 0.90$ suggested by Allsop et al. (1994) for $R_c/H_{m0} > 1$. Numerical results also confirm that R_c/H_{m0} has almost no influence on the reflection coefficients for traditional breakwaters with high relative crest freeboard ($R_c/H_{m0}>1$). Fig. 4 shows that K_r values obtained for the innovative caisson are lower than those for the traditional one, ranging between 0.56 and 0.76. Therefore, when OBREC-V is inserted K_r is reduced up to 40% in comparison to the values computed for the traditional vertical breakwater. These lower values were expected due to the energy dissipation when waves interact with the non-conventional geometry of the superstructure. As for the traditional caisson, the relative crest freeboard, R_c/H_{m0}, has a small influence on K_r.

The influence of the ramp crest freeboard, R_r, and the position of the crown-wall, B_{wall}, on the reflection coefficients is also analysed. Fig. 5 consists of nine panels, one for each of the different incident wave conditions tested in this analysis (Table 1). Each row displays results for different peak periods increasing from left to right. Each column displays results for increasing wave height. The numerical values of K_r for each B_{wall} and R_r are also shown.

Fig. 5 clearly indicates that K_r increases with R_r for all the tested wave conditions. This is due to the larger amounts of small non-overtopped waves that are directly reflected from the ramp with the increase of its freeboard, leading to an increase of the (bulk) reflection coefficient. On the other hand, the influence of the B_{wall} is less evident, although a general trend can be noted with a slight reduction of K_r with the increase of B_{wall}, in particular, for tests with higher significant wave heights (bottom panels in Fig. 5). Indeed, when waves interact with the large reservoir, high turbulence levels occur inside the reservoir, thus high amount of the energy from incoming waves is dissipated and a reduction of K_r is measured. More evident is the influence of the energetic period $T_{m-1,0}$, and so the wavelength based on this period, $L_{-1,0}$. For each row on Fig. 5, the reflection coefficient increases from left to right panels, indicating that for the same significant wave height, K_r

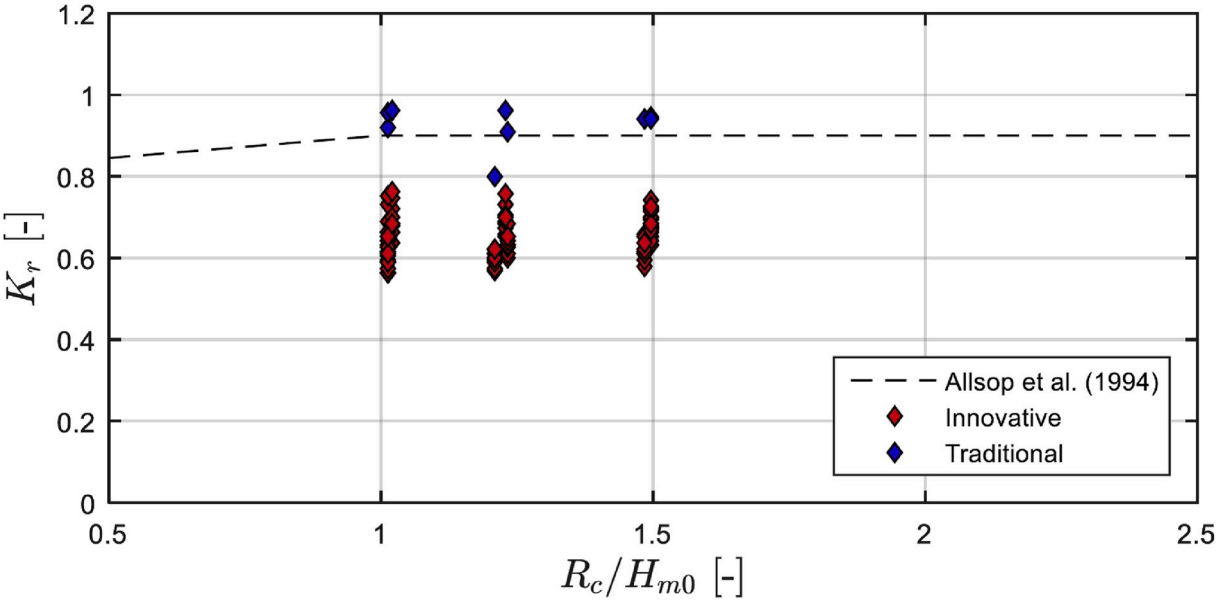

Fig. 4. Numerical reflection coefficients for traditional and innovative caisson compared with the formula from Allsop et al. (1994).

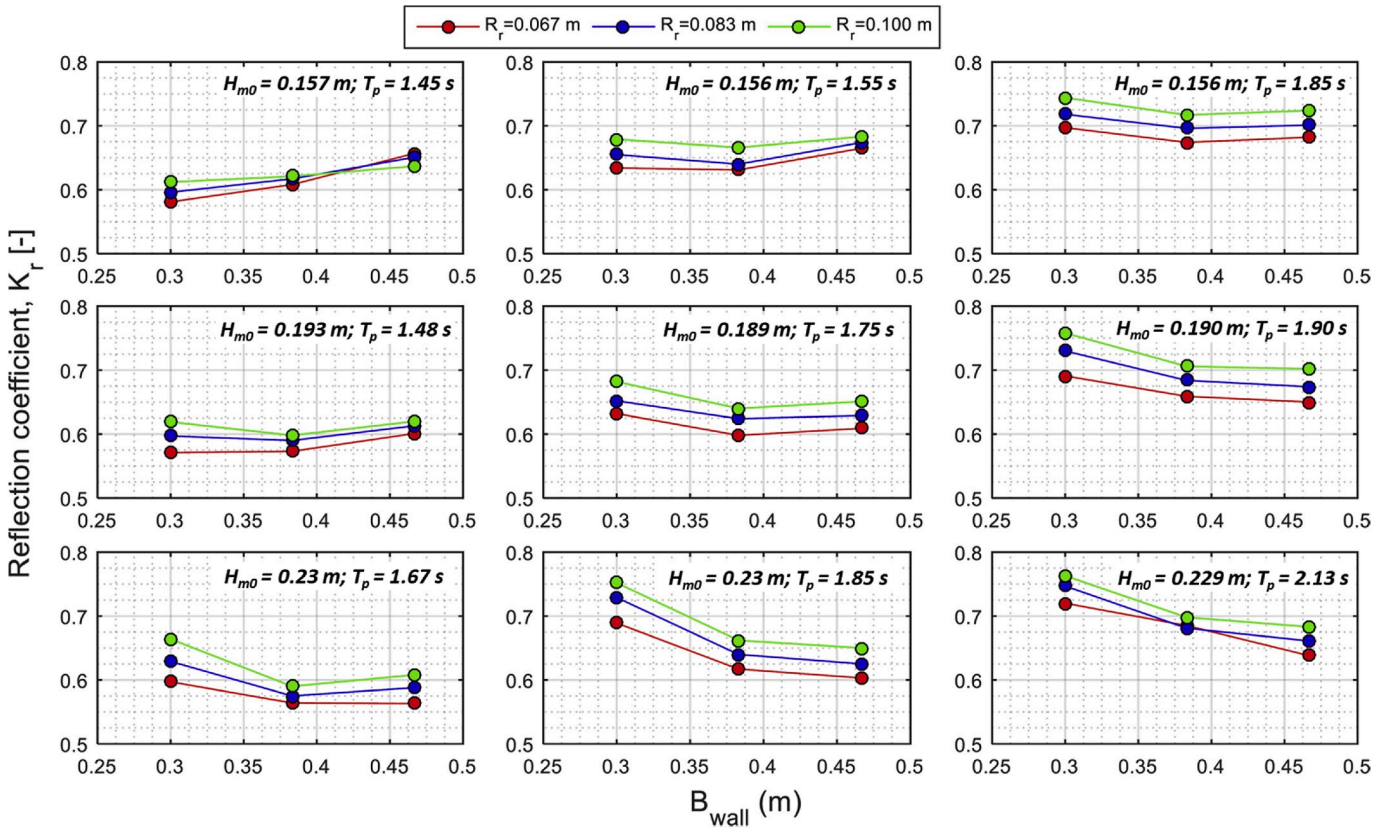

Fig. 5. Influence of crown-wall position B_{wall} and crest ramp R_r on the reflection coefficient K_r, for the nine wave conditions.

increases with the increase of $L_{-1,0}$, i.e. the effect of the OBREC-V device on the reduction of the reflection is mitigated when the structure interacts with long waves.

Fig. 6 shows how the reflection coefficients decrease with the increase of the non-dimensional parameter $(B_{wall}/L_{-1,0})/(R_r/H_{m0})$, which considers the aforementioned parameters that influence reflection. The

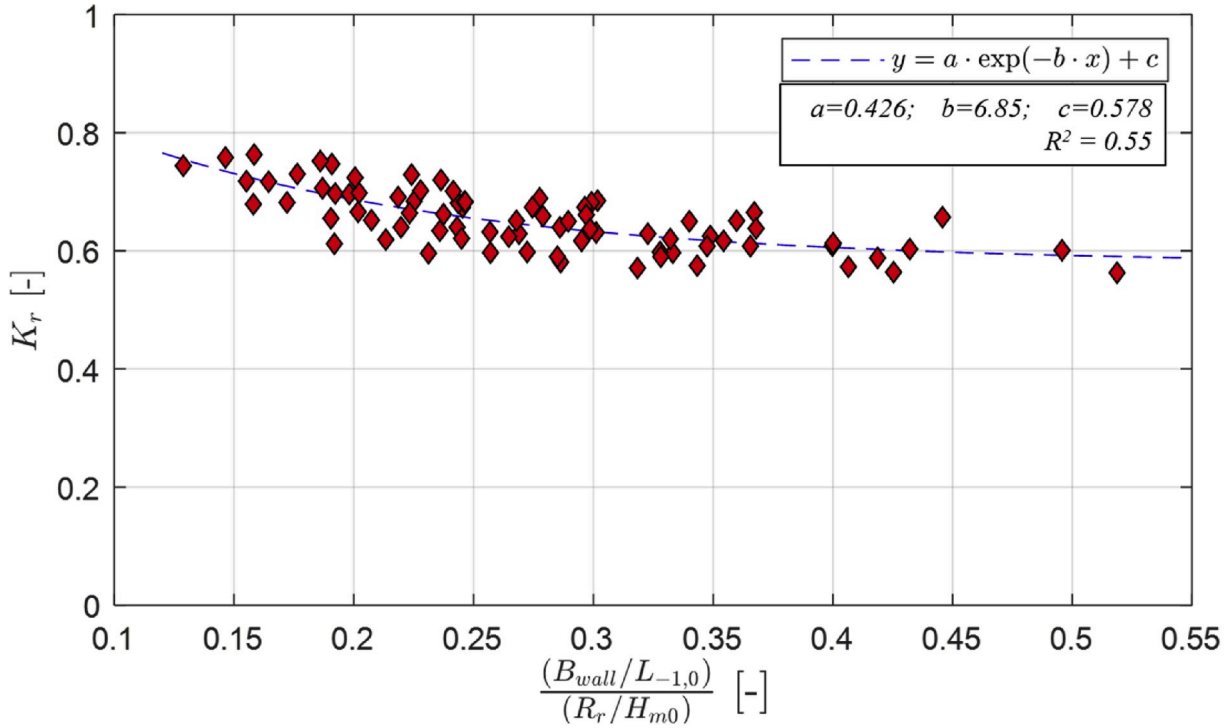

Fig. 6. Reflection coefficients obtained from the numerical model for the OBREC caisson breakwater, function of the relative ramp crest, R_r/H_{m0}, and relative vertical wall position, $^{B/L}_{wall-1,0}$

points fit reasonably well to an exponential law, whose coefficients are evaluated fitting the data with a non-linear least square method. The reflection coefficient on the OBREC-V can be derived with the following relation:

$$K_{r,OBREC-V} = a \cdot exp \cdot \left[- b \cdot \frac{(B_{wall}/L_{-1,0})}{(R_r/H_{m0})} \right] + c \quad (1)$$

The value of the correlation coefficient R^2 is equal to 0.55 and the empirical coefficients in Eq. (1) are: a = 0.426, b = 6.85 and c = 0.578. Although the obtained R^2 is not high, the root-mean-square error (RMSE) calculated between the observed K_r and the values predicted by the relation proposed in this work is equal to 0.033. This value is similar to the RMSE error found in literature for the prediction of the reflection coefficients for typical coastal structures (CIRIA, CUR, CETMEF, 2007). Please note that Eq. (1) is valid for the parameters range indicated in Table 2.

3.2. Wave overtopping

3.2.1. Influence of the geometric parameters

To evaluate the advantage of the numerical tool to provide a sensitivity analysis of the influence of the geometrical parameters of the OBREC-V to the wave overtopping discharge, an analysis of the wave overtopping discharge over the crown-wall of the traditional breakwater and the OBREC-V was done. The use of identical wave generation signals, for each of the different caisson configurations, allows comparing not only the mean wave overtopping discharge, q, per unit of length ($m^3/s/m$), but also to compare the cumulated wave overtopping volume per unit of length (m^3/m) on the time domain. The wave overtopping data was calculated only for three wave conditions: *Test_02*, *Test_05* and *Test_08*, for a total of 40 tests. An example is displayed in Fig. 7 for *Test_05*, showing the cumulative wave overtopping volume for the same incident wave condition and 10 different geometries. Left panels show the influence of the relative set-back crown-wall position, $B_{wall}/L_{-1,0}$, for each different relative ramp crest, R_r/H_{m0}. Right panels show the influence of R_r/H_{m0} for each different relative position of the set-back wall, $B_{wall}/L_{-1,0}$. Black dashed lines are displayed in each panel, indicating the numerical results of the cumulative wave overtopping discharge at the rear side of the traditional vertically-faced structure. The different configurations have the same wall crest dimension (R_c = 0.183 m).

Results indicate a reduction in wave overtopping volume with increasing $B_{wall}/L_{-1,0}$, confirming that the position of the set-back wall is an important factor to consider for the OBREC-V design. Large values of B_{wall} lead to higher energy dissipation of the waves that overtop the ramp and break into the stilling basin, thus causing a significant reduction of wave overtopping over the innovative caisson. The results were expected, considering the performance of the OBREC-R device presented by Iuppa et al. (2016), where wave overtopping was found to decrease with the increase of the horizontal distance between the crown-wall and the crest of the ramp. The results shown in the right panels of Fig. 7 indicate a minor influence of R_r/H_{m0} on the overtopping volume. In general, higher ramp crest results in higher wave overtopping values. As for the OBREC-R (Contestabile et al., 2017b), the frontal ramp in the OBREC-V works as a deflector, conducting the water jet on the exposed part of the set-back wall, especially for short B_{wall} values.

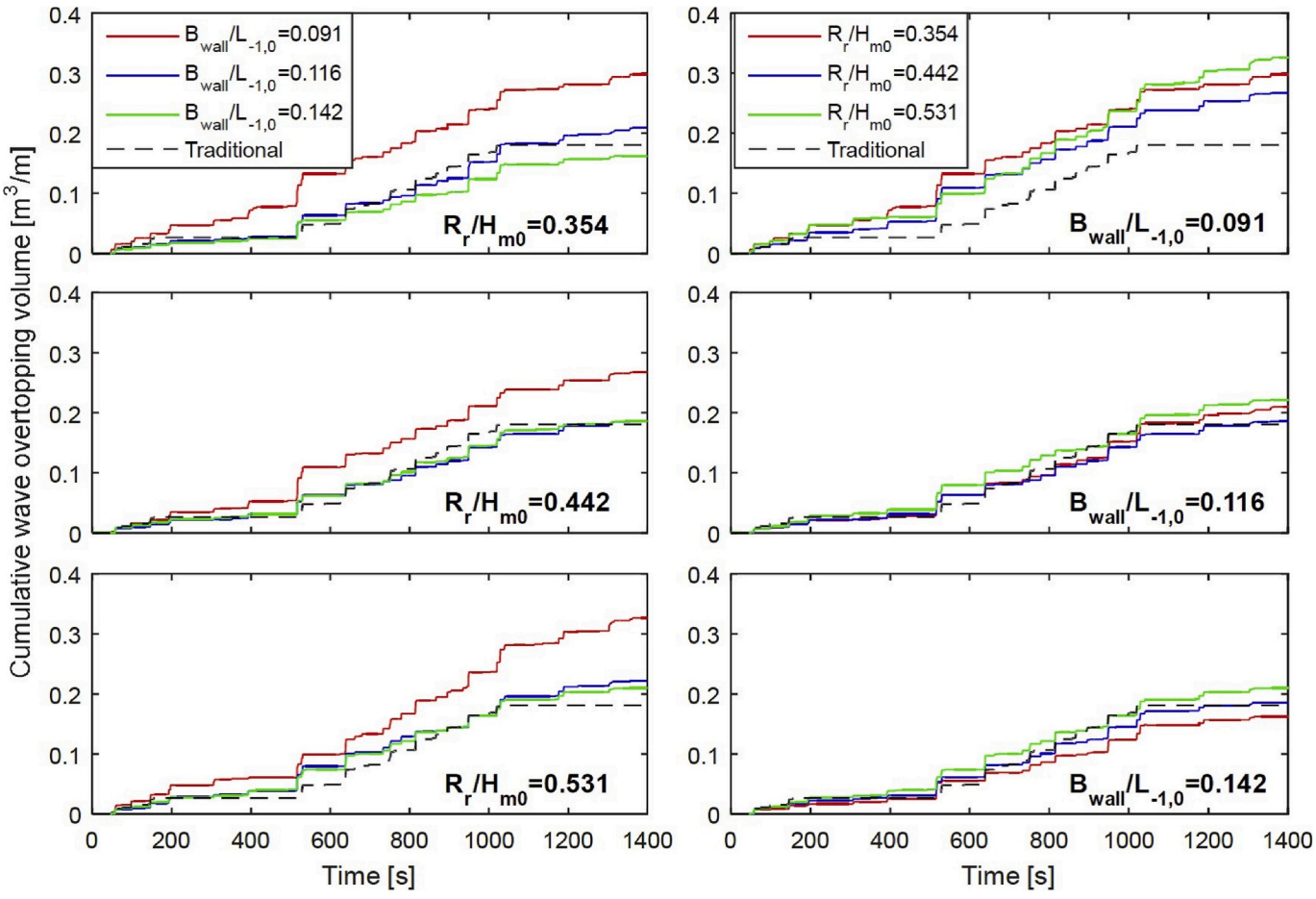

Fig. 7. Influence of the relative ramp crest, R_r/H_m0, and relative vertical wall position, $B_{wall}/L_{-1,0}$, on the cumulative wave overtopping volume for *Test_05*.

3.2.2. Comparison between innovative and traditional caissons

A further step in the wave overtopping analysis is to compare the numerical results to the formula adopted in the EurOtop Manual (EurOtop, 2016) to estimate the mean wave overtopping discharge over the vertical and steep walls. In absence of physical models, the EurOtop Manual can be considered the most reasonable tool for a preliminary calculation of the overtopping discharge on traditional breakwaters.

As previously described, the numerical model tests are carried out in a domain characterized by a flat bottom in front of the structures, and wave conditions close to deep water limits (Hofland et al., 2017). Under these conditions, shoaling and depth limiting effects on the spectral shape along the numerical domain can be negligible. Therefore, the results of the numerical analysis are compared to the equation of EurOtop Manual for wave overtopping discharge over vertical walls with '*no influencing foreshore*':

$$\frac{q}{\sqrt{g \cdot H_{m0}^3}} = 0.047 \cdot \exp\left[- \left(2.35 \frac{R_c}{H_{m0}} \right)^{1.3} \right] \quad (2)$$

The empirical coefficients of the exponential formula are derived from measured data and the reliability of the relationship is given by $\sigma(0.047) = 0.007$ and $\sigma(2.35) = 0.23$, where σ is the standard deviation of the parameter and the coefficients between brackets are mean values, μ, of the parameters. Fig. 8 displays the numerical results of nondimensional wave overtopping discharge for traditional and innovative caissons. The numerical data are compared to Eq. (2) in the EurOtop Manual. The 5% under and upper exceedance limits (= 90%-confidence band) are displayed in Fig. 8 with blue dotted lines, calculated by using $\mu(x) \pm 1.64 \cdot \sigma(x)$ for the two empirical coefficients.

Results show that the numerical data of mean wave overtopping for traditional and innovative breakwater match to Eq. (2) with a high level of accuracy. As can be seen from Fig. 8, almost all the data are contained in the 90%-confidence band of Eq. (2). Differences are more evident for high values of relative crest freeboard, where the scatter between data are higher due to the low amount of wave overtopping discharge. Results indicate that differences between the various configurations are very small. For preliminary design purpose Eq. (2) can be used to estimate the wave overtopping discharge at the rear side of the OBREC-V. In fact, wave overtopping is strongly dependent on the maximum height of the parapet, rather than on its position, as already observed by Benassai (1984), who studied the wave overtopping behaviour on breakwaters with crown-wall located away from the leading edge of the caisson. Similar results were obtained by Kisacik et al. (2019), who studied the effect of the SWB for overtopping reduction at an urban vertical seawall.

However, as shown in the previous section, the variation of $B_{wall}/L_{-1,0}$ leads to differences between the numerical results of mean wave overtopping on innovative caisson and those estimated using Eq. (2). To predict the mean overtopping with higher accuracy, an influence factor, named γ_{OBREC}, is then introduced into Eq. (2) to take into account the innovative geometry of the OBREC-V. The approach followed in the analysis is similar to the one adopted in the EurOtop manual (EurOtop, 2016) for the reduction coefficients γ in the wave overtopping equations. The equation turns into:

$$\frac{q}{\sqrt{g \cdot H_{m0}^3}} = 0.047 \cdot \exp\left[- \left(2.35 \frac{R_c}{H_{m0} \cdot \gamma_{OBREC}} \right)^{1.3} \right] \quad (3)$$

The values of γ_{OBREC} are plotted in Fig. 9 in terms of $B_{wall}/L_{-1,0}$, which is the dominating parameter. The data fit relatively well ($R^2 = 0.70$) with the following exponential law:

$$\gamma_{OBREC} = 1.163 \cdot \exp\left(- 1.737 \frac{B_{wall}}{L_{-1,0}} \right) \quad (4)$$

Then, relative overtopping is evaluated using equations (3) and (4). Fig. 10 shows a good performance of the modified overtopping formula considering the new parameter, γ_{OBREC}.

4. Wave loading: forces and stability analysis

The analysis of the loadings and the stability analysis of the OBREC-V

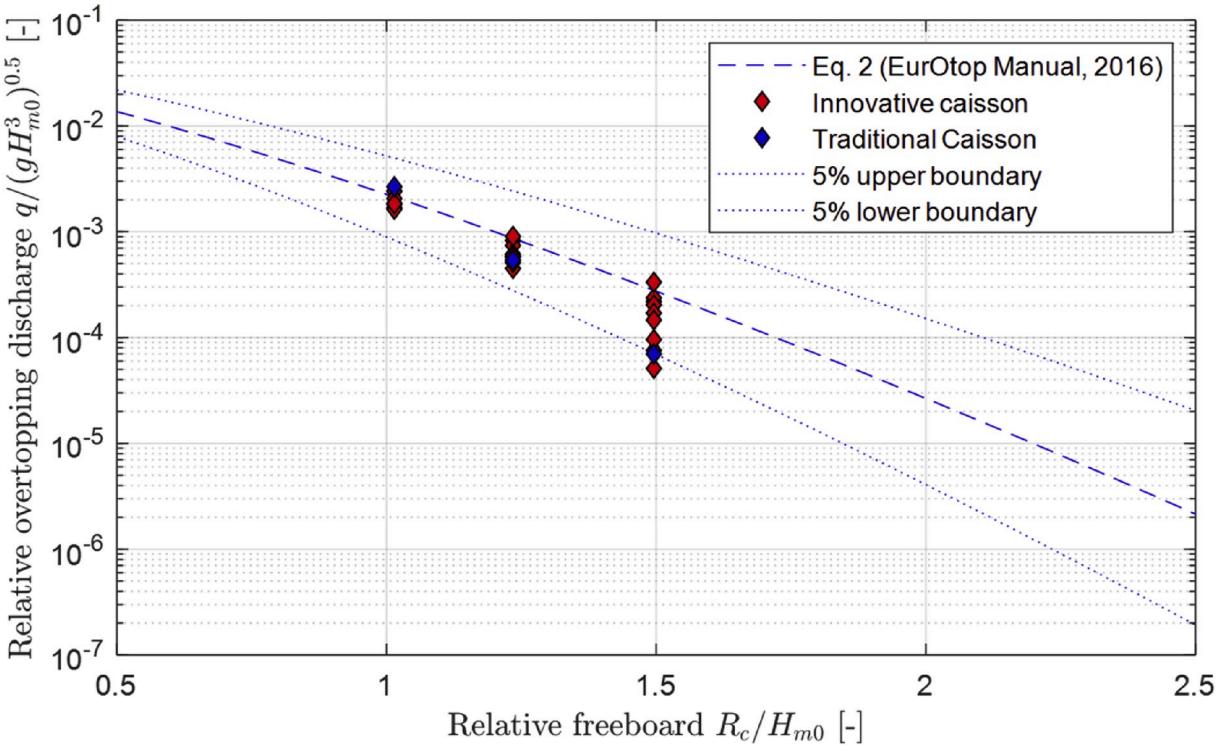

Fig. 8. Measured numerical data of the wave overtopping discharges over the traditional (blue points) and the innovative OBREC caisson (red points). Wave overtopping equation for vertical breakwater (Eq. 7.1 in EurOtop, 2016) with 5% under and upper exceedance limits is reported with blue dotted lines. (For interpretation of the references to colour in this figure legend, the reader is referred to the Web version of this article.)

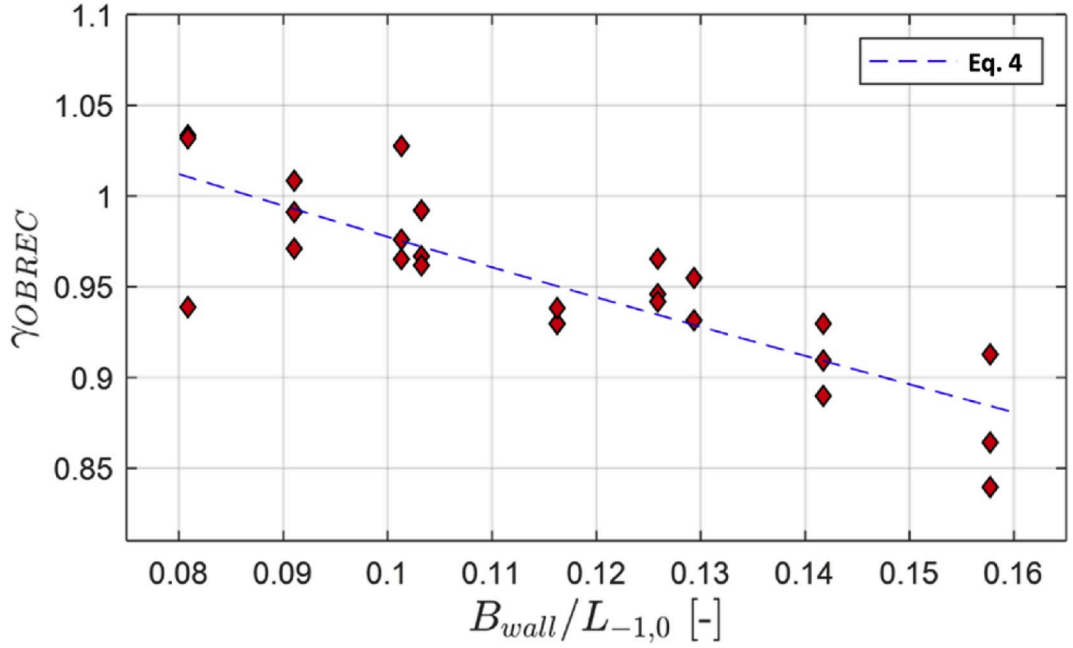

Fig. 9. Calculated γ_{OBREC} as a function of the relative vertical wall position, $^{B/L}_{wall-1,0}$.

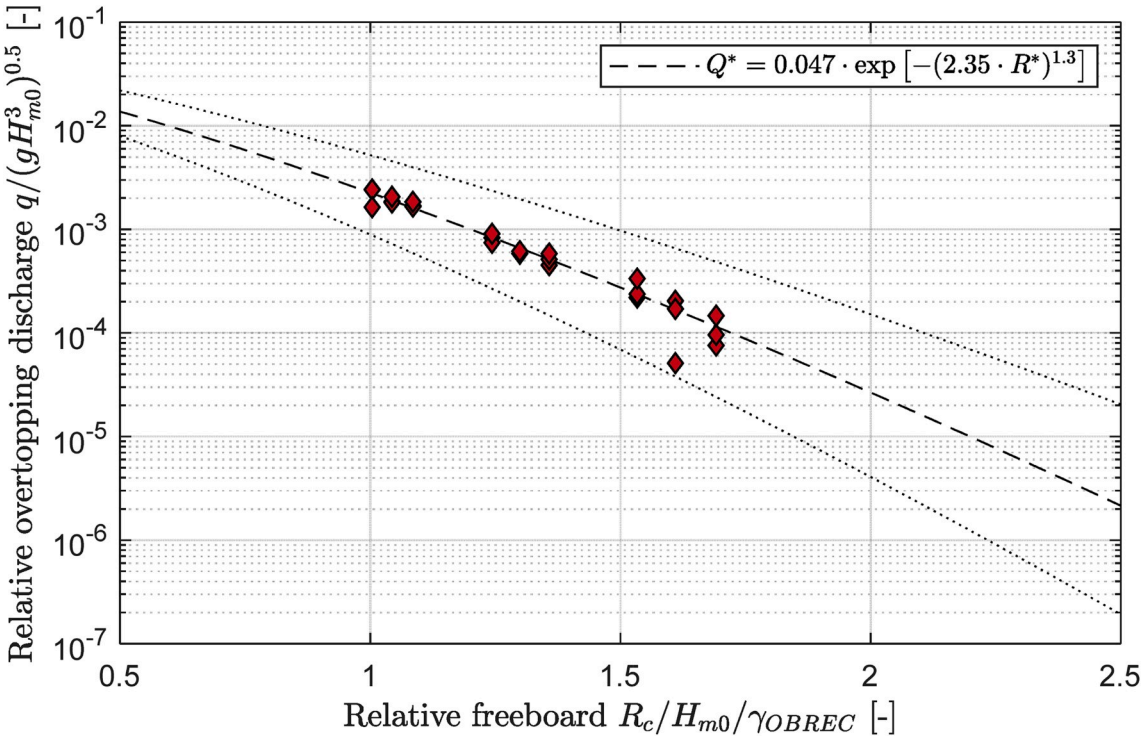

Fig. 10. Numerical data points of the wave overtopping compared to the formula from EurOtop Manual corrected with the coefficient γ_{OBREC} to take into account the OBREC geometry.

is evaluated in a similar way to the one described by Di Lauro et al. (2019) for the numerical analysis of the OBREC-R. The analysis is carried out considering the forces based on the average of the highest 1/250th peaks of the forces in a given random sequence, denoted as $F_{1/250}$. The local maxima (peaks) of the force signal evaluated in a specific part of the structure are extracted by considering a minimum time window between peaks equal to $T_{m,02}$. This time window is considered to take into account only the local force peak for each single incident wave. Moreover, to avoid the inclusion of the signal with small peaks in the computation part, each local peak event is extracted considering a high-pass threshold that varies depending on the wave conditions and the part of the structure on which the pressure is integrated. The threshold used in the peak-extraction analysis is equal to $0.1\rho_w g H_{m0} L_x$, where L_x is the length of the structure on which the pressure is integrated. Please note that the resultant wave forces are calculated assuming a linear pressure distribution between the dynamic pressures numerically calculated in each cell.

A sketch of the differences between wave pressure distribution and

forces exerted on the traditional and innovative caisson is displayed in Fig. 11. The figure also indicates how the total vertical ($F_{v,OBREC}$) and horizontal forces ($F_{h,OBREC}$) exerted on the innovative caisson are calculated, taking into account the loading on the vertical frontal face caisson, $F_{h,OBREC,\ caisson}$, the ramp, $F_{OBREC,\ ramp}$, the bottom reservoir, $F_{v,\ OBREC,res}$, the base caisson, $F_{v,OBREC,\ base}$, and the vertical wall, $F_{h,OBREC,\ wall}$. The horizontal and vertical forces exerted on the traditional vertically-faced structure are indicated as $F_{h,trad}$ and $F_{v,trad}$, respectively.

4.1. Wave loads compared to the Goda formulas

The first part of the present analysis is aimed at comparing the force exerted on the traditional caisson to the design formula usually adopted for design purpose. In the absence of physical model tests, the empirical formulas in literature are the most reliable tool for the calculation of wave forces on traditional vertical structures. The most adopted method for the evaluation of the force exerted on a vertical caisson is the one described by Goda (2010), in which a trapezoidal pressure distribution along the vertical wall and a triangular distribution on the base are assumed. Please observe that the ratio between the depth above the armour layer of the rubble foundation and the water depth in front of the breakwater, d/h, is equal to 0.82 for all tests. Therefore, the correction proposed by Takahashi (1994) does not change the magnitude of the pressure calculated by using Goda formulas, i.e. no impulsive wave pressure condition occurs for the tests here considered. Furthermore, as indicated in Table 2, $Hm0/h < 0.35$, which further excludes the presence of impulsive waves on vertical breakwater according to the 'Parameter Map' for the prediction of impact forces in the PROVERBS (Oumeraci et al., 2001).

Fig. 12 shows the comparison of the horizontal (left panel) and vertical forces (right panel) between the values calculated with the Goda formulas and the forces ($F_{1/250}$) calculated on the vertical breakwater with the numerical model. The mean and standard deviation of the deviation are also displayed, defined as the difference between the forces calculated with Goda formula minus the ones calculated numerically, divided by the former values. These deviations are expressed in percentages and calculated for each one of the nine numerical tests carried out on traditional vertically-faced structures. Results indicate a general good match between the data, with a slight overestimation of the horizontal force of 13.7% and an underestimation of the uplift force exerted on the structure of 12.5%. The overall results can be considered satisfactory, bearing in mind the level of uncertainty associated with these semi-empirical formulas (Juhl and Van der Meer, 1992; Bruining, 1994; Van der Meer et al., 1995; Oumeraci et al., 2001; Agerschou, 2004). For instance, Van der Meer et al. (1995) presented the results of the ratio between the forces (horizontal and vertical) computed with Goda method and those measured in laboratory for different geometries and wave conditions with irregular waves, indicating a very large scatter of the results. Please note that the widely adopted Goda formulas were originally proposed after performing laboratory tests using regular waves (Goda and Fukumori, 1972; Goda, 1973). This can explain the slight discrepancies, when results of tests carried out adopting irregular waves are compared with Goda formulas. This fact has been recently supported by Castellino et al. (2018) who showed a better agreement with Goda formulas when regular waves are considered in the analysis.

4.2. Wave forces on traditional and innovative caisson

The forces exerted on the traditional and innovative caissons were analysed investigating the influence of the two geometrical parameters B_{wall} and R_r. Numerically computed forces on the innovative caissons are compared to the ones obtained for the traditional one.

Fig. 13 shows the influence of the relative ramp crest, R_r/H_{m0}, and the relative crown-wall position, $B_{wall}/L_{-1,0}$, on the ratio between the horizontal forces exerted on the innovative and traditional caisson, $F_{h,\ OBREC}/F_{h,trad}$. Dotted black lines are included in the panels, indicating the condition where the total horizontal forces between the two different caisson configurations are equal. The left panel in Fig. 13 indicates that the ratio between innovative and traditional caisson is not influenced by

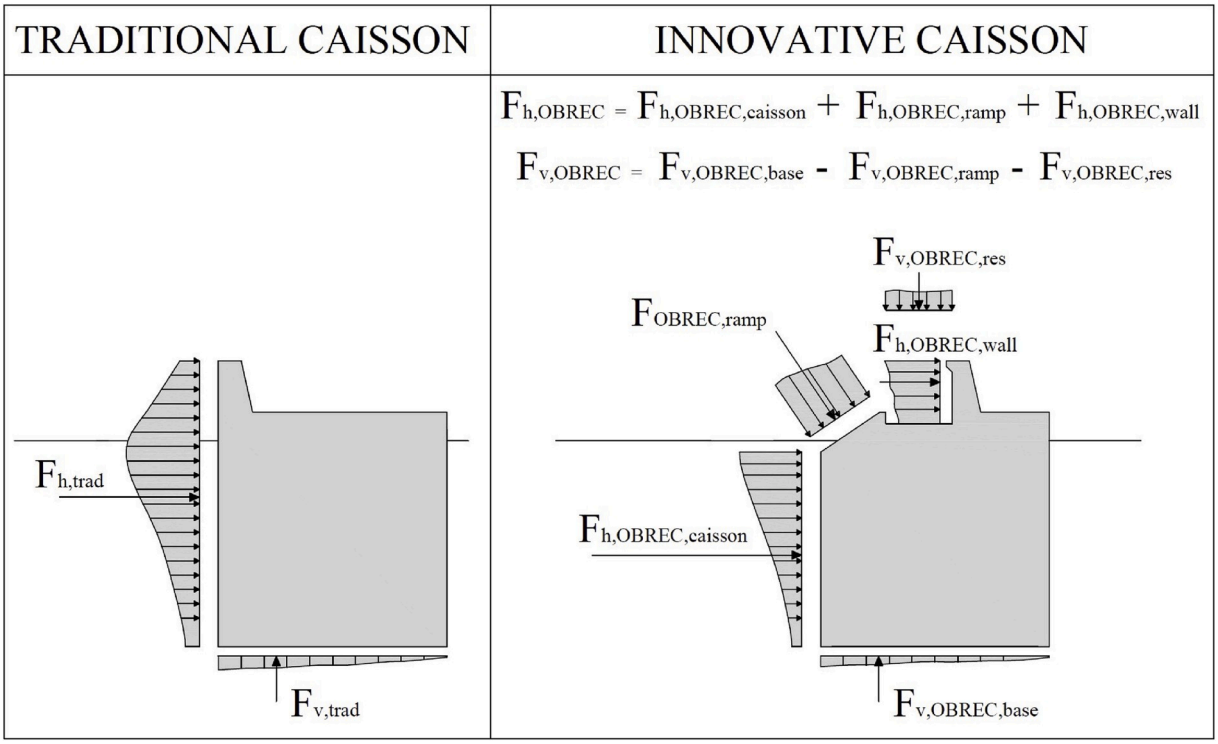

Fig. 11. Sketch of the wave pressure distribution and forces exerted on traditional vertical breakwater (left panel) and innovative caisson integrated with the OBREC device (right panel).

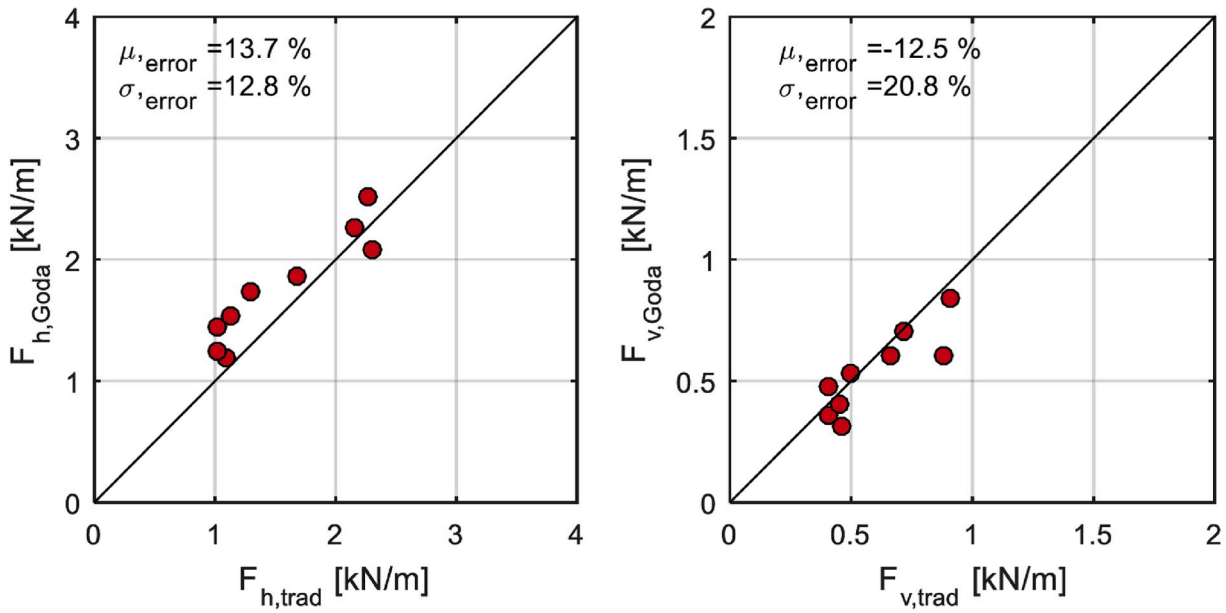

Fig. 12. Comparison between the numerical horizontal (left panel) and vertical forces (left panel) on traditional breakwater with those computed with Goda formulas (Goda, 2010).

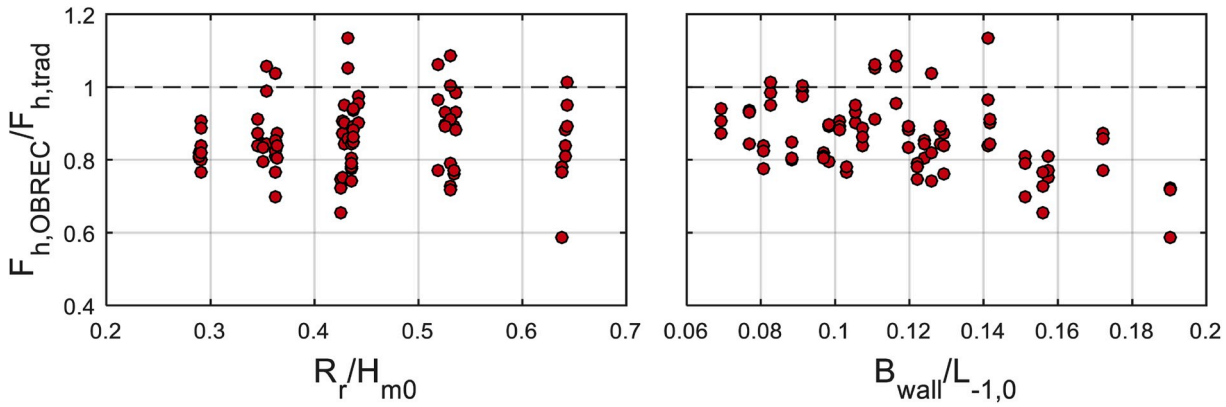

Fig. 13. Influence of the relative ramp crest R_r/H_{m0} (left panel) and the relative wall position $B_{wall}/L_{-1,0}$ (right panel) of the ratio between the total horizontal forces exerted on the innovative and traditional caisson, $F_{h,OBREC}/F_{h,trad}$.

R_r/H_{m0}. Contrary, the increase of the ratio $B_{wall}/L_{-1,0}$ leads to a slightly reduction of the $F_{h,OBREC}$ compared to the one calculated on the vertical caisson (right panel). As presented in previous sections, the increase of $B_{wall}/L_{-1,0}$ leads to a reduction of overtopping over the OBREC-V crown-wall. The reduction of the overtopping does not cause an increase of the total force on the structure, due to the energy dissipation of the waves that overtop the ramp and break in the reservoir. Furthermore, as will be shown in the next sections, the position of the set-back crown-wall in the OBREC-V influences the time lag between the maximum force peaks acting on the caisson and on the wall. Therefore, the increase of the B_{wall} further reduces the maximum total horizontal peak forces exerted on the innovative breakwater, compared to the traditional one. Furthermore, results indicate that higher reduction of the force occurs with incident waves characterized by small peak periods. Conversely, as explained in the previous section, long waves are less influenced by the presence of the OBREC device embedded on the caisson, leading to only a slight reduction of the horizontal forces compared to the ones computed on the vertically-faced structure. Results shown in Fig. 13 clearly indicate that the total horizontal forces exerted on the innovative caisson are, for most of the analysed cases, lower than the ones calculated on the vertical breakwaters, with a reduction up to 40%. It is worth nothing that these results are similar to the ones obtained by Oumeraci et al. (1993) on a caisson with a vertically lower part with semi-cylindrical shells that terminates with a plane slope on the top upper part. Authors calculate a reduction of the horizontal impact forces between 30 and 60% compared to the vertical flat front, depending on the prevailing waves and depth conditions. Similar results have been recently obtained by Misra et al. (2011). Authors conducted a numerical analysis on the Civitavecchia breakwater, characterized by a particular superstructure with curved and recessed parapet, compared to a traditional vertical structure. Results indicated that the use of the non-conventional geometry at the Civitavecchia breakwater reduces the total landward forces of around 20% compared to the ones computed on a vertical structure.

Fig. 14 displays the influence of R_r/H_{m0} and $B_{wall}/L_{-1,0}$ on the ratio between the total vertical forces exerted on the innovative and traditional caisson $F_{v,OBREC}/F_{v,trad}$. The two panels in Fig. 14 show that $F_{v,OBREC}/F_{v,trad}$ is reduced with the increase of R_r/H_{m0} (left panel) and $B_{wall}/L_{-1,0}$ (right panel). As expected, the introduction of the OBREC device on vertical caissons induces a relevant reduction of vertical forces due to the downward components exerting on the ramp and the bottom reservoir. Furthermore, the wave energy dissipation inside the reservoir

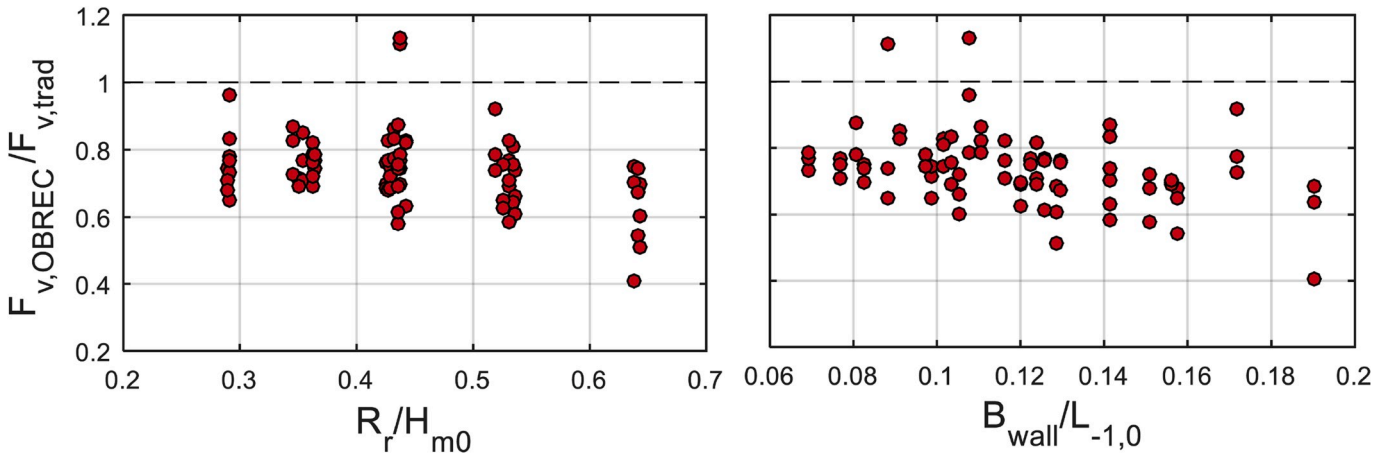

Fig. 14. Influence of the relative ramp crest R_r/H_{m0} (left panel) and the relative wall position $B_{wall}/L_{-1,0}$ (right panel) of the ratio between the total vertical forces exerted on the innovative and traditional caisson.

reduces further the total forces on the structure. Results confirmed the importance of the B_{wall} on the reduction of the overall vertical forces. The increase of B_{wall} leads to a reduction of the ratio $F_{v,OBREC}/F_{v,trad}$ for all the tests. Moreover, higher values of the ramp crest freeboard R_r lead to a higher downward (stabilizing) forces, thus reducing the ratio $F_{v,OBREC}/F_{v,trad}$.

The same is observed for increasing $B_{wall}/L_{-1,0}$ values. Then, the overall stability is increased with the inclusion of the innovative structure.

4.3. Forces on the set-back wall

A set-back parapet on the top of vertical breakwaters has been adopted in the past as a solution to reduce the impact pressure exerted on the caisson superstructure and its effect on the breakwater stability. The *Duca degli Abruzzi* breakwater in Naples, the breakwater at the Civitavecchia Harbour in Rome, and the dike in Bagnara (Franco, 1992) are examples of breakwaters in Italy with capping walls set back with respect to the wall profile. Although the importance of this non-conventional superstructure, scarce literature regarding the pressure and forces exerted on it exists.

Benassai (1984) and Van der Meer and Benassai (1985) investigated the wave pressure and forces on a small model reproducing different cross-sections of the breakwater proposed for the extension of the Civitavecchia Harbour in Italy. Local impact pressures on the set-back parapet were measured and different shapes of the signals were classified in schematic diagrams. Pressure signals on the structure were characterized by an oscillatory nature, which is influenced by the compression of the air-pocked trapped between the wave and the parapet. Benassai (1984) demonstrated that the superstructure influenced the vertical slamming forces, which in turn has a relevant effect on the structure stability. Madrigal and Alarcon (1992) demonstrated that a set-back wall does not contribute to the total wave load on the structure, because the forces exerted on it are out of phase with respect to the forces on the main vertical profile. The overall stability is increased due to the reduction of forces caused by the delay in wave action on the two surfaces and due to the prevention of impulsive breaking wave conditions caused by wave discontinuity. Regarding this aspect, the Italian Standards (National Research Council, 1994) suggest that the set-back superstructure must be verified assuming that the maximum pressures exerted on it are given by the Hiroi formulas ($p = 1.5\ \rho_w g H$).

In this section, the numerical results of the horizontal forces exerted on the set-back wall of the innovative caisson are investigated. Please note that the height of the wall, i.e. the vertical distance between its crest and the internal bottom reservoir, a_{wall}, is constant and equal to 0.183 m (see Fig. 3) for all tests. Moreover, the water depth, h, is also constant; hence, the crown-wall has the same values of crest freeboard R_c. Consequently, the various wall configurations are obtained with a horizontal translation of the wall, assuming a constant distance to the water level. Fig. 15 shows how the nondimensional horizontal force on the wall, $F_{h,OBREC,\ wall}/(\rho_w g H_{m0} a_{wall})$, varies with the ratio between the significant wave height and the water depth, H_{m0}/h. Results clearly indicate a pronounced linear dependency between the nondimensional forces on the wall and the ratio H_{m0}/h. The behaviour is similar to that observed by many authors (Jensen, 1984; Pedersen, 1996) that studied the resultant force exerted on crown-wall placed on the top of rubble-mound breakwaters. As can be observed in Fig. 15, the average pressure on the wall (i.e. $F_{h,OBREC,\ wall}/a_{wall}$), ranges between 0.7 and 2.5 times $\rho_w g H_{m0}$, while R_r and B_{wall} are not dominant variables in the resulting forces. The force on the wall can be derived with the following relation:

$$\frac{F_{h,OBREC,wall}}{g H_{m0} a_{wall}} = a\left(\frac{H_{m0}}{h}\right) + b \tag{5}$$

The value of the correlation coefficient R^2 is equal to 0.75 and the empirical coefficients in Eq. (5) are: $a = 10.15$ and $b = -1.45$.

The characteristics of the wave loading on the set-back wall are evaluated considering the time series of the forces exerted on it, where the occurrence of impact loads cannot be completely excluded. Fig. 16 shows, on the upper panel, an example of the time series of the nondimensional wave force exerted on the set-back wall ($F_{h,OBREC,\ wall}/\rho_w g H_{m0}$) for *Test_08* with $R_r = 0.067$ m and $B_{wall} = 0.300$ m. The signal shows rapid variations in time, with force peaks typically described as impact wave loads with absence of trapping air. The so-called '*church-roof*' shape of the force signal can be recognized, as the ones occurred for breaking waves on vertical structures (Oumeraci et al., 2001). On the bottom panels of Fig. 16, nondimensional wave pressure distributions ($p/\rho_w g H_{m0}$) along the crown-wall are displayed for seven time instants. These instants are chosen as representative ones including the one corresponding to the maximum force on the set-back wall ($t = 435.866$ s) for this specific test. Please observe that the reference system for the pressure distribution indicated on the seven bottom panels of Fig. 16 has its origin on the bottom part of the wall pointing on the tip of the wall, as indicated on the right part of the upper panel.

As can be observed in Fig. 16, the pressure on the set-back wall exhibits impact pressure, with p_{max} around 6 $\rho g H_{m0}$. It is worth noting that the pressure signals, especially on the upper part of the crown-wall, have relatively small peak pressure if compared to the general pressure peaks for violent impact loads on vertical walls, which can be up to 50 $\rho g H_{m0}$ at the still water level, as shown by many authors (Schmidt et al., 1993; Hattori et al., 1994; Allsop et al., 1997; Oumeraci et al., 2001; Bullock

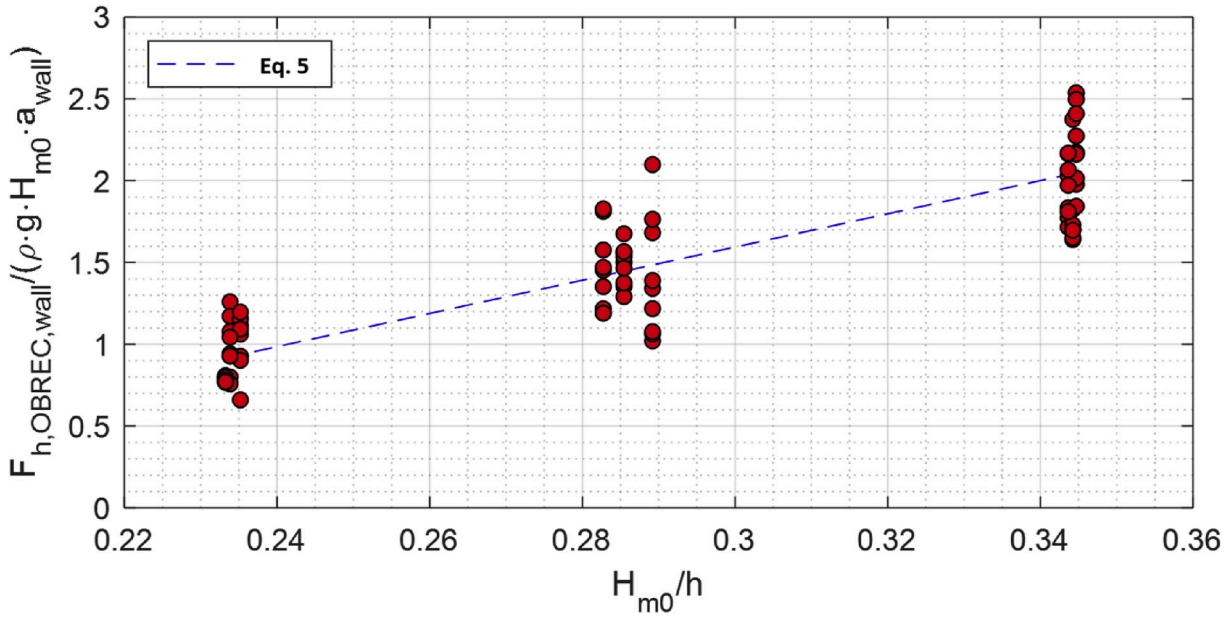

Fig. 15. Influence of H_{m0}/h on the non-dimensional force exerted at the set-back wall.

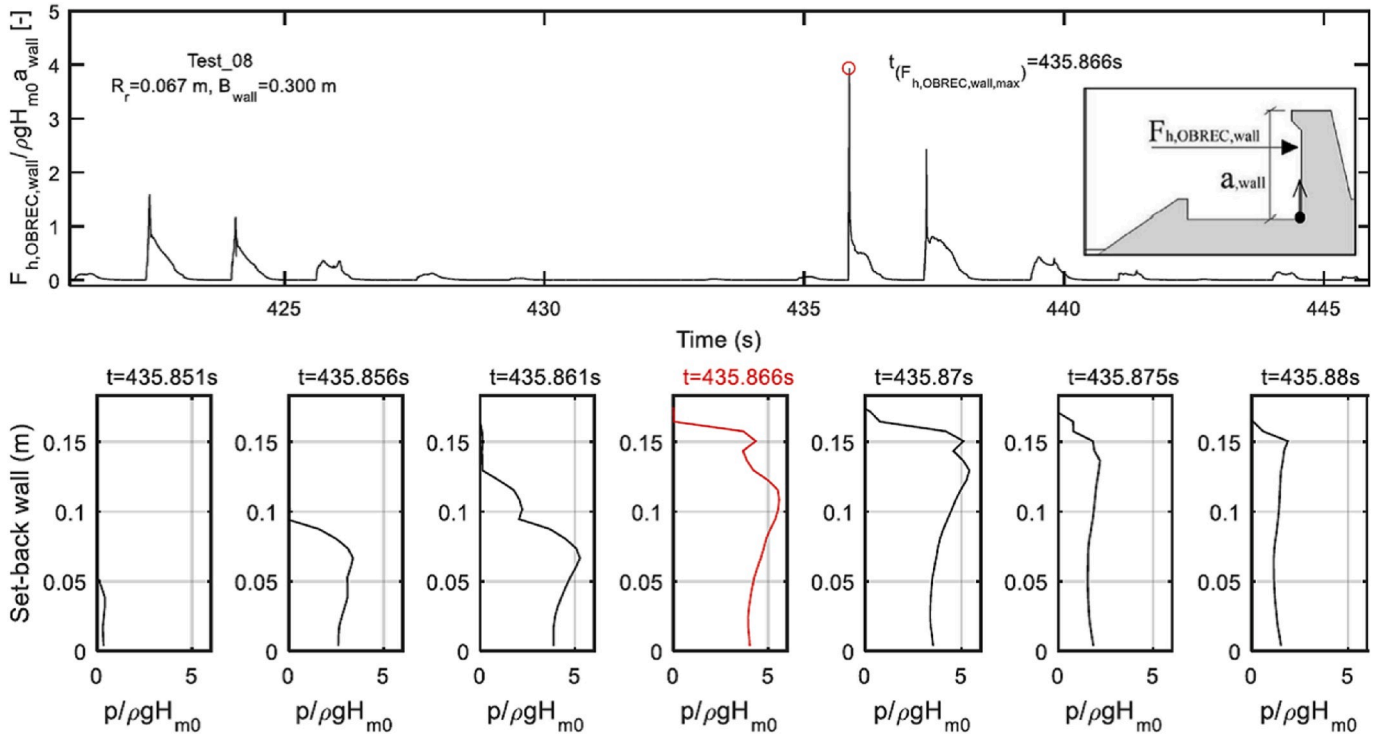

Fig. 16. Time series of the nondimensional wave forces, $F_{h,OBREC,\ wall}/\rho_w g H_{m0} a_{wall}$, exerting on the set-back wall (upper panel) and nondimensional wave pressure distribution, $p/\rho_w g H_{m0}$, along the wall for seven representative time instants (bottom panels) for *Test_08* with R_r = 0.067 m B_{wall} = 0.300 m.

et al., 2007). The energy dissipation due to wave run-up over the ramp and on the reservoir greatly attenuates the pressure peaks, as already recognized by Vicinanza et al. (2014) and Contestabile et al. (2017b) on test campaign conducted on the OBREC-R.

4.4. Stability analysis

The design of a vertical breakwater requires a stability analysis of the caisson and its foundation. In detail, the caisson must be designed to be safe against sliding and overturning. Moreover, the hydraulic stability and bearing capacity of the rubble-mound foundation and the seabed need to be investigated, considering that geotechnical failure may lead to the stability loss of the caisson situated on it. It is customary to evaluate the bearing capacity of the foundation using the traditional methodology in geotechnical engineering, with a foundation subjected to inclined and eccentric loads produced by the weight of the upright section and wave forces. In coastal engineering, the overturning around the caisson heel has been traditionally considered as an overall failure mode of the structure. This method implicitly makes the assumption of a rigid foundation below the structure. However, in most cases, sliding is

more severe than overturning, especially when the breakwater crest is relatively low. Indeed, the most common modes of failure caused by wave load due to plunging breakers are sliding, shear failure on the foundation, but rarely overturning (Goda, 1973; Oumeraci et al., 1993; Takahashi, 2002; Agerschou, 2004). The overturning is often a direct consequence of the hydraulic instability and failure of the yielding foundation. The traditional design procedure against the overturning of the caisson is considered by many authors (see for example Oumeraci et al., 1993; Agerschou, 2004) too simplistic and unrealistic as it does not take into account the loss of the bearing capacity and the capacity failure of the rubble-mound and sub-soil foundation. For the over-mentioned reasons, only the stability of the caisson against sliding on the rubble-mound foundation is considered.

The safety factor of the traditional and innovative caisson against sliding over the foundation, C_s, is computed as:

$$C_S = \frac{\mu\,(Mg - F_v)}{F_h} \tag{6}$$

where μ is the coefficient of (static) friction between the base caisson and the rubble foundation, F_h and F_v are the resulting overall horizontal and vertical wave forces numerically calculated on the innovative and traditional caisson as shown in Fig. 11; M is the mass of the monolithic structure per unit extension, including the sand fill and superstructure; and g is the acceleration due to the gravity. In the present analysis, the friction coefficient is assumed to be 0.6, while the mass densities of the caisson, ρ_c, could be assumed, based on classical design, to be 2.1 t/m^3 for the sand-filled caisson and 2.3 t/m^3 for the concrete superstructure. For the submerged part of the caisson, a mass density of 1.1 t/m^3 is considered. For the two configurations, the sand-filled caisson is assumed to be extended until 0.05 m (1.5 m in prototype scale) above the SWL.

The time series of the safety factors against sliding, C_s, for the traditional and innovative caisson are analysed for each test. Please note that, contrary to the statistical analysis of the resultant horizontal and vertical forces, C_s is here considered as the minimum value during the test. The minimum C_s occurs at the instant of the maximum destabilizing forces, F_s, defined as:

$$F_s = F_h + \mu F_v \tag{7}$$

Fig. 17 consists of nine panels, indicating the different incident wave conditions tested in this analysis (Table 1). In detail, the peak period increases from left to right panels, while the wave height increases from top to bottom panels of each column. Each panel displays the values of C_s for different values of B_{wall} and R_r. Horizontal red dotted-lines are included in each panel, indicating the numerical values of C_s calculated on the traditional vertically-faced structure.

Then, values of C_s computed for the innovative caisson are similar or greater than those calculated on the vertical structure for almost all the tests. The non-conventional geometry of the innovative caisson integrated with an OBREC device increases, in general, the overall stability of the structure compared to traditional breakwaters. The results confirm the behaviour already described when comparing the resultant forces on the caissons. In particular, the relevant component of the downward force on the superstructure and the time lag between the vertical and horizontal forces, lead to a strong reduction of the maximum destabilizing forces F_s in the innovative breakwater, whose values range between the 60–80% of the ones computed on the traditional structure.

Contrary to the analysis on the forces, the minimum C_s is not always obtained for the highest peak periods. The resultant forces at the instant of the minimum value of C_s strongly depend on the period of a single wave, more than on the spectral peak period of the generated wave

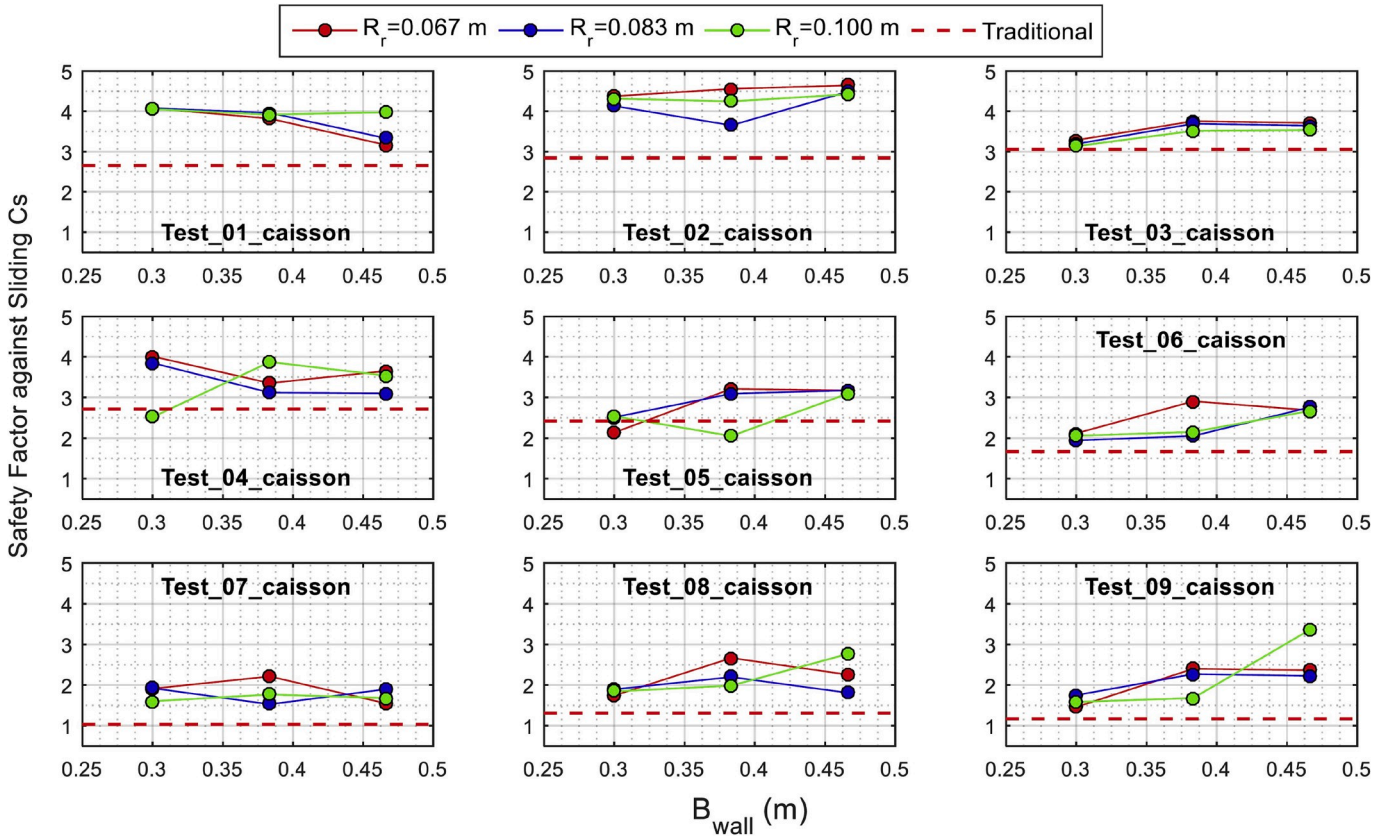

Fig. 17. Influence of crown-wall position B_{wall} and crest ramp R_r on the safety factor against sliding, C_s, for the nine wave conditions. Red dotted-lines indicate the numerical values of C_s calculated on the traditional vertical structure. . (For interpretation of the references to colour in this figure legend, the reader is referred to the Web version of this article.)

train. Regarding the position of the crown-wall, it can be seen that similar behaviour described for the total forces can be replied here, particularly for tests characterized by large significant wave height (bottom panels in Fig. 17). C_s is similar to the one calculated on a vertical structure and, in general, it increases with higher values of B_{wall}. Results indicate also that the ramp crest R_r has no relevant influence on the safety factor C_s.

An example of the time series of the resultant horizontal (F_h), vertical (F_v) and destabilizing forces (F_s) is shown in Fig. 18 for *Test_08*. Three configurations of the innovative breakwater with different B_{wall} and a fixed ramp crest ($R_r = 0.067$ m) are compared to the traditional structure. The case shown in Fig. 18 (the one from Fig. 16) is characterized by the occurrence of sporadic impact loadings on the set-back wall, in particular for the condition with $B_{wall} = 0.300$ m. The top panel in Fig. 18 indicates a different behaviour between the total horizontal forces on the traditional breakwater and the innovative caisson. Due to the presence of the set-back wall, each signal of the innovative caissons is characterized by two distinctive peaks. The maximum horizontal forces for each wave occurs when the wave impacts on the set-back wall (second peak), while the first peaks are in phase with those computed for the traditional breakwater, but they are shorter in magnitude due to the energy dissipation caused by the wave overtopping over the frontal ramp. The central panel in Fig. 18 shows the signals of the total vertical forces exerted on the four different configurations. The vertical forces on the innovative breakwater increase until reaching a maximum value, which is in phase and with similar magnitude of the one computed on the traditional breakwater. After this peak, the vertically downward component of the force exerted on the sloping ramp and the reservoir drastically reduces the total vertical forces on the innovative breakwater. It can be noted in this panel how the dimension of the reservoir influences the vertical forces on the caisson, i.e. the increase in B_{wall} leads to a decrease in the total vertical forces. Contrary to the traditional breakwater, the maximum vertical and horizontal forces exerted on the innovative breakwater occur at different time steps, whose time lag increase with B_{wall}. Then, the total destabilizing forces F_s (Eq. (7)) differ from the ones found for the traditional caisson. The bottom panel of Fig. 18 shows these results. This example clearly indicates that an innovative caisson having a crest freeboard and caisson width equal to the one of a traditional structure is characterized by a similar or greater stability, even for the conditions when an impact wave loading occurs on the set-back wall (red lines in Fig. 18 for $B_{wall} = 0.300$ m). For cases with a larger B_{wall}, the destabilizing forces are smaller than the ones for a traditional caisson.

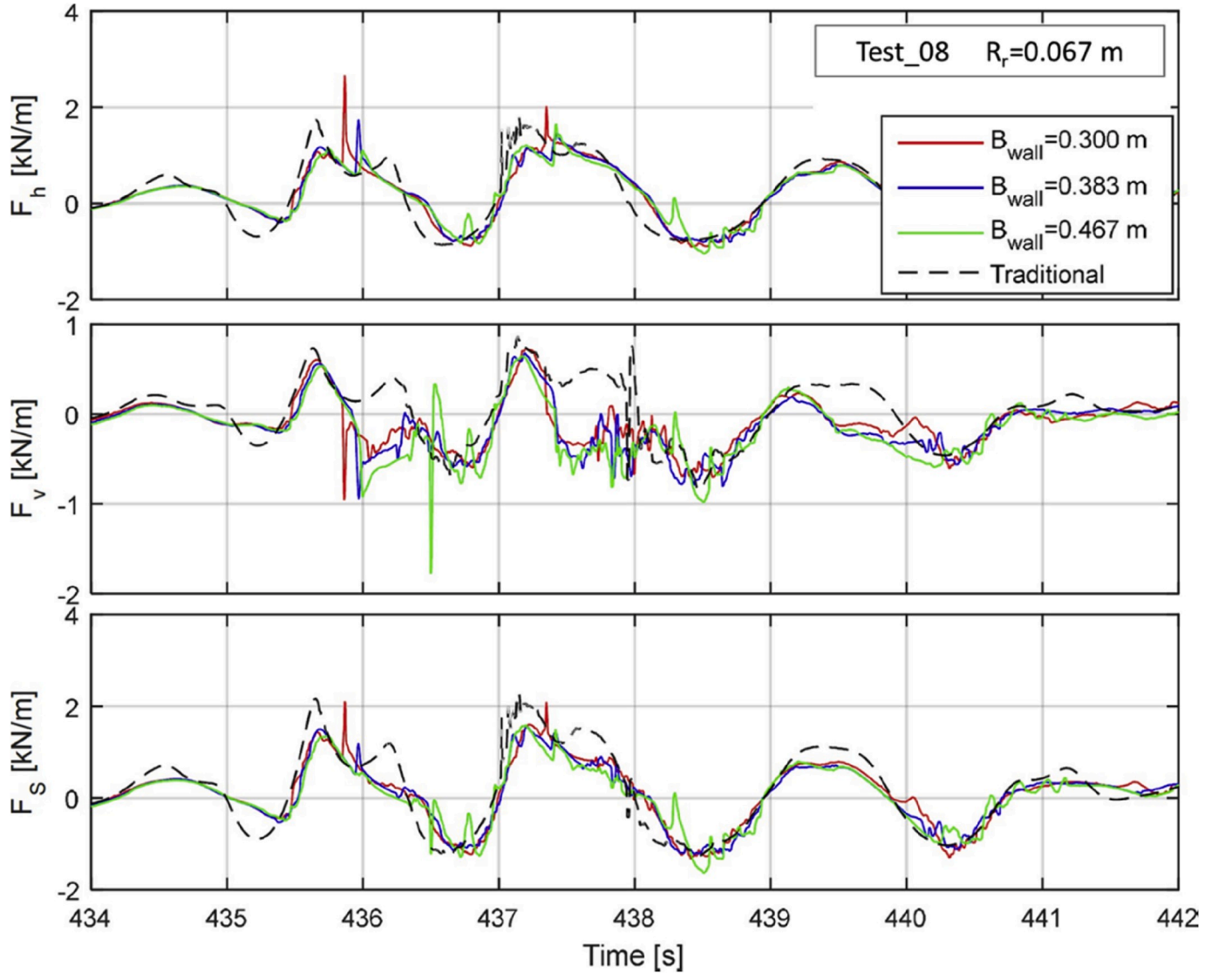

Fig. 18. Time series of the total horizontal (top panel) and vertical force (middle panel) on traditional and innovative caisson with a fixed value of crest ramp ($R_r = 0.067$ m) for *Test_*08. Bottom panel indicates the time series of the total destabilizing force, F_S.

5. Conclusions

The hydraulic performance and structural stability of an innovative vertical breakwater with an overtopping wave energy converter was investigated using the IH2VOF numerical model (Losada et al., 2008; Lara et al., 2011), extensively validated by Di Lauro et al. (2019) against physical model tests on OBREC-R. The numerical modelling was applied to study the interaction between irregular waves and traditional and innovative vertical caissons, comparing the results in terms of wave reflection, overtopping and resultant wave forces exerted on the structures. A total of 90 numerical model tests have been carried out in the present analysis.

Numerical simulations were performed on different OBREC-V configurations, allowing to investigate the influence of the ramp crest freeboard, R_r and the position of the set-back wall, B_{wall}, on the hydraulic performance, as well as their effects on the global caisson stability. Numerical results obtained on the innovative breakwater were then compared with those obtained on a vertical caisson with the same wall crest freeboard and caisson width. Results indicate that the integration of the OBREC device in a traditional vertically-faced structure has numerous advantages in terms of hydraulic and stability analysis.

Due to the wave dissipation on the ramp and reservoir, the reflection coefficients computed in front of the OBREC-V are lower than those computed in front of the traditional vertical breakwater, with a reduction of up to the 40%. An empirical relation, function of the relative crest freeboard R_r/H_{m0} and the relative wall position $B_{wall}/L_{-1,0}$, is provided in this paper to estimate the reflection coefficients for different incident wave conditions and OBREC-V configurations. The reduction of wave reflection is obtained under extreme wave conditions. Under milder waves, this reduction would be lower since only few waves are expected to overtop the frontal ramp. Therefore, under those conditions, K_r is expected to be similar to the ones obtained for the traditional vertical breakwater.

Regarding wave overtopping, results of the average and cumulative wave overtopping discharge behind the set-back wall of the innovative breakwater indicate that it significantly depends on the distance between the wall and the vertical face of the caisson, B_{wall}. In detail, the increase of B_{wall} reduces wave overtopping for all the incident wave conditions analysed. The comparison between traditional and innovative caisson show that the mean wave overtopping discharge for the different configurations match the equation suggested in the EurOtop Manual (EurOtop, 2016) for vertical structures, and almost all the numerical data are contained in the 90%-confidence band of this equation. However, to predict the mean overtopping discharge for the OBREC-V with higher accuracy, a new coefficient was proposed in order to adapt the application of the equation proposed in EurOtop Manual taking into account the non-conventional geometry of the OBREC-V.

The resultant vertical and horizontal wave forces exerted on traditional and innovative breakwaters were also investigated for the stability analysis. Regarding the horizontal forces, results indicate that the ratio between the forces exerted on innovative and traditional caisson is not influenced by R_r/H_{m0}. Contrary, the increase of the ratio $B_{wall}/L_{-1,0}$ leads to a slight reduction of the $F_{h,OBREC}$ compared to the one calculated on the vertical breakwater $F_{h,trad}$. In fact, the resultant horizontal forces on the set-back wall occur later than those on the front wall, with a reduction of the total horizontal forces on the whole structure. Therefore, the increase of B_{wall} leads to a reduction of the ratio $F_{h,OBREC}/F_{h,trad}$ for almost all the tests here analysed. Results indicate also that long waves are less influenced by the presence of the OBREC device installed on the caisson, leading to only a slight reduction compared to the total forces computed on the traditional vertically-faced structure. In detail, for the highest value of T_p and the lowest value of B_{wall}, the performance of the two configurations in terms of total horizontal wave forces are comparable.

Regarding the total vertical forces, results show that the ratio $F_{v,OBREC}/F_{v,trad}$ is reduced with the increase of R_r/H_{m0} and $B_{wall}/L_{-1,0}$. As expected, the introduction of the OBREC device on vertical caissons induces a reduction of vertical forces due to the significant downward components exerted on the ramp and the bottom reservoir. Furthermore, wave energy dissipation inside the reservoir reduces further the forces on the structure. For higher values of R_r/H_{m0} and $B_{wall}/L_{-1,0}$ the downward force on the OBREC-V is half of the vertical uplift exerted on the base caisson. The analysis of the loads exerted on the different configurations clearly underlines the advantage of adopting this novel solution with non-conventional shape due to the increase of the stability compared to the traditional structure.

Finally, results show that the non-conventional geometry of the innovative caisson integrated with an OBREC device highly increases the overall stability of the structure. The values of the safety factor against sliding, C_s (Eq. (6)) computed for innovative caissons are similar or greater than those calculated for the vertical structure for almost all the tests, confirming the behaviour described for the resultant forces on the innovative and traditional caisson. In particular, the component of the downward force on the superstructure and the time lag between the vertical and horizontal forces, lead to a significant reduction of the maximum destabilizing forces F_s (Eq. (7)) in the innovative breakwater, whose values range between the 60–80% of the ones computed on the traditional structure.

This study highlights the hydraulic and stability differences between the OBREC-V and a traditional vertical breakwater. The OBREC-V entails higher construction costs, but it also entails a set of co-benefits that must also be considered in a decision-making process when designing a new vertical breakwater. These co-benefits include not only the inherent energy production of the device itself, but also the decreased wave reflection and greater hydraulic stability compared to a traditional design under the same wave conditions.

Declaration of competing interest

The authors declare that they have no known competing financial interests or personal relationships that could have appeared to influence the work reported in this paper.

CRediT authorship contribution statement

Enrico Di Lauro: Conceptualization, Methodology, Investigation, Formal analysis, Validation, Writing - original draft. **Maria Maza:** Methodology, Investigation, Writing - review & editing. **Javier L. Lara:** Methodology, Writing - review & editing, Supervision. **Inigo J. Losada:** Writing - review & editing, Supervision. **Pasquale Contestabile:** Conceptualization. **Diego Vicinanza:** Conceptualization, Supervision.

Acknowledgements

This article was supported by the OCEANERA-NET project, SE@PORTS (Sustainable Energy at Sea PORTS), reference OCEANERA/0003/2016, under the frame of Sociedad para el Desarrollo Regional de Cantabria S.A. – SODERCAN. Authors gratefully acknowledge the Doctoral School of Environment, Design and Innovation at *Università degli Studi della Campania "Luigi Vanvitelli"* - Department of Engineering for supporting researchers mobility. M. Maza is indebted to the Spanish Ministry of Science, Innovation and Universities for the funding provided in the grant Juan de la Cierva Incorporación (BOE de 27/10/2017).

References

Cappietti, L., Aminti, P.L., 2012. Laboratory investigation on the effectiveness of an overspill basin in reducing wave overtopping on marina breakwaters. In: Proceedings of 33rd Conference on Coastal Engineering. Santander, Spain, 2012.

Agerschou, H., 2004. Planning and Design of Ports and Marine Terminals. Thomas Telford Publishing, ISBN 0727732242.

Allsop, W., McBride, M., Colombo, D., 1994. The reflection performance of vertical walls and low reflection alternatives: results of wave flume tests. In: Proceedings of the 3rd MCS Project Workshop, MAS2-CT92-0047, Monolithic (Vertical) Coastal Structures. De Voorst, The Netherlands.
Allsop, N., McKenna, J., Vicinanza, D., Whittaker, T., 1997. New design methods for wave impact loadings on vertical breakwaters and seawalls. Coast. Eng. 2508–2521, 1996.
Benassai, E., 1984. Some considerations on design of vertical wall breakwater. In: International Symposium on "Maritime Structures in the Mediterranean Sea (Athens).
Bruining, J., 1994. Wave Forces on Vertical Breakwaters: Reliability of Design Formula. Master's thesis. Delft University of Technology.
Bullock, G., Obhrai, C., Peregrine, D., Bredmose, H., 2007. Violent breaking wave impacts. part 1: results from large-scale regular wave tests on vertical and sloping walls. Coast. Eng. 54 (8), 602–617.
Burcharth, H.F., Andersen, T.L., 2007. Overtopping of rubble mound breakwaters with front reservoir. In: Coastal Engineering 2006. World Scientific, pp. 4605–4615 (In 5 Volumes).
Castellino, M., Sammarco, P., Romano, A., Martinelli, L., Ruol, P., Franco, L., De Girolamo, P., 2018. Large impulsive forces on recurved parapets under non-breaking waves. A numerical study. Coast. Eng. 136, 1–15.
Contestabile, P., Ferrante, V., Di Lauro, E., Vicinanza, D., 2017a. Full- scale prototype of an overtopping breakwater for wave energy conversion. In: Proceedings of 35th Conference on Coastal Engineering. Antalya, Turkey, 2016.
Contestabile, P., Iuppa, C., Di Lauro, E., Cavallaro, L., Andersen, T.L., Vicinanza, D., 2017b. Wave loadings acting on innovative rubble mound breakwater for overtopping wave energy conversion. Coast. Eng. 122, 60–74.
CIRIA, CUR, CETMEF, 2007. The Rock Manual. The use of rock in hydraulic engineering., , 2nd editionC683. CIRIA, London.
Contestabile, P., Crispino, G., Di Lauro, E., Ferrante, V., Gisonni, C., Vicinanza, D., 2019. Overtopping Breakwater for wave Energy Conversion: review of state of art, recent advancements and what lies ahead. Renew. Energy 147, 705–718.
Di Lauro, E., Lara, J.L., Maza, M., Losada, I.J., Contestabile, P., Vicinanza, D., 2019. Stability analysis of a non-conventional breakwater for wave energy conversion. Coast. Eng. 145, 36–52.
EurOtop, Van der Meer, J.W., Allsop, N.W.H., Bruce, T., De Rouck, J., Kortenhaus, A., Pullen, T., Schuttrumpf, H., Troch, P., Zanuttigh, B., 2016. Manual on Wave Overtopping of Sea Defences and Related Structures. An Overtopping Manual Largely Based on European Research, but for Worldwide Application. www.overtopping-manual.com.
Franco, L., 1992. Recent Italian Experience in the Design and Construction of Vertical Breakwaters. Design and Reliability of Coastal Structures, Short Course during the 23rd ICCE in Venice.
Geeraerts, J., De Rouck, J., Beels, C., Gysens, S., De Wolf, P., 2007. Reduction of wave overtopping at seadikes: stilling Wave Basin (SWB). In: Coastal Engineering 2006. World Scientific, pp. 4680–4691 (In 5 Volumes).
Goda, Y., 1973. A new method of wave pressure calculation for the design of composite breakwaters. Rep. Port Harbour Res. Inst. 12 (3), 31–69.
Goda, Y., 2010. Random seas and design of maritime structures. World Sci. 732.
Goda, Y., Fukumori, T., 1972. Laboratory investigation of wave pressures exerted upon vertical and composite walls. Coast. Eng. Japan 15, 81–90.
Guanche, R., Losada, I.J., Lara, J.L., 2009. Numerical analysis of wave loads for coastal structure stability. Coast. Eng. 56 (5–6), 543–558.
Hasselmann, K., Barnett, T., Bouws, E., Carlson, H., Cartwright, D., Enke, K., Ewing, J., Gienapp, H., Hasselmann, D., Kruseman, P., et al., 1973. Measurements of wind-wave growth and swell decay during the joint North Sea wave project (JONSWAP). Ergänzungsheft 8–12.
Hattori, M., Arami, A., Yui, T., 1994. Wave impact pressure on vertical walls under breaking waves of various types. Coast. Eng. 22 (1–2), 79–114.
Hofland, B., Chen, X., Altomare, C., Oosterlo, P., 2017. Prediction formula for the spectral wave period Tm-1, 0 on mildly sloping shallow foreshores. Coast. Eng. 123, 21–28.
Iuppa, C., Contestabile, P., Cavallaro, L., Foti, E., Vicinanza, D., 2016. Hydraulic performance of an innovative breakwater for overtopping wave energy conversion. Sustainability 8 (12), 1–20.
Jensen, O.J., 1984. A Monograph on Rubble Mound Breakwaters. Danish Hydraulic Institute (DHI).
Juhl, J., Van der Meer, J., 1992. Quasi-static Wave Forces on Vertical Structures, Reanalysis of Data at Danish Hydraulic Institute and Delft Hydraulics Report. Prepared for MAST G6-S Coastal Structures.
Kisacik, D., Tarakcioglu, G.O., Baykal, C., 2019. Stilling wave basins for overtopping reduction at an urban vertical seawall–The Kordon seawall at Izmir. Ocean Eng. 185, 82–99.
Lara, J., Losada, I., Guanche, R., 2008. Wave interaction with low-mound breakwaters using a rans model. Ocean Eng. 35 (13), 1388–1400.
Lara, J.L., Ruju, A., Losada, I.J., 2011. Reynolds Averaged Navier–Stokes modelling of long waves induced by a transient wave group on a beach. In: Proceedings of the Royal Society of London A: Mathematical, Physical and Engineering Sciences, vol. 467. The Royal Society, pp. 1215–1242.
Losada, I.J., Lara, J.L., Guanche, R., Gonzalez-Ondina, J.M., 2008. Numerical analysis of wave overtopping of rubble mound breakwaters. Coast. Eng. 55 (1), 47–62.
Losada, I.J., Lara, J.L., del Jesus, M., 2016. Modeling the interaction of water waves with porous coastal structures. J. Waterw. Port, Coast. Ocean Eng. 142 (6).
Madrigal, B.G., Alarcon, J.J., 1992. Influence of superstructure geometry on the behaviour of vertical breakwaters: two case studies. PIANC Bull. 76.
Misra, S., Narayanaswamy, M., Bayram, A., Shi, F., 2011. Optimization of caisson breakwater superstructure geometry using a 2dv RANS-VOF numerical model. Coast. Eng. Proc. 1 (32), 49.
National Research Council, 1994. Technical instruction for the design of maritime dikes. Pubbl. GNDCI n 1450.
Oumeraci, H., Klammer, P., Partenscky, H., 1993. Classification of breaking wave loads on vertical structures. J. Waterw. Port, Coast. Ocean Eng. 119 (4), 381–397.
Oumeraci, H., Kortenhaus, A., Allsop, W., de Groot, M., Crouch, R., Vrijling, H., Voortman, H., 2001. Probabilistic Design Tools for Vertical Breakwaters. CRC Press.
Palma, G., Mizar Formentin, S., Zanuttigh, B., Contestabile, P., Vicinanza, D., 2019. Numerical simulations of the hydraulic performance of a breakwater-integrated overtopping wave energy converter. J. Mar. Sci. Eng. 7 (2), 38.
Pedersen, J., 1996. Wave Forces and Overtopping on Crown Walls of Rubble Mound Breakwaters: an Experimental Study. Ph.D. thesis. Aalborg University.
Rosa-Santos, P., Taveira-Pinto, F., Clemente, D., Cabral, T., Fiorentin, F., Belga, F., Morais, T., 2019. Experimental study of a hybrid wave energy converter integrated in a harbor breakwater. J. Mar. Sci. Eng. 7 (2), 33.
Schaffer, H.A., Klopman, G., 2000. Review of multidirectional active wave absorption methods. J. Waterw. Port, Coast. Ocean Eng. 126 (2), 88–97.
Schmidt, R., Oumeraci, H., Partenscky, H.-W., 1993. Impact loads induced by plunging breakers on vertical structures. In: Proceedings of the 23rd International Conference on Coastal Engineering, pp. 1545–1558. October 4-9, 1992, Venice, Italy.
Takahashi, S., 1994. A proporsal of impulsive pressure coefficient for design of composite breakwater. In: Proceedings of the International Conference on Hydro-Technical Engineering for Port and Harbor Construction,, vol. 1, pp. 489–504, 1994.
Takahashi, S., 2002. Design of Vertical Breakwaters. PHRI Reference Document, vol. 34.
Uihlein, A., Magagna, D., 2016. Wave and tidal current energy–A review of the current state of research beyond technology. Renew. Sustain. Energy Rev. 58, 1070–1081.
Van der Meer, J., Benassai, E., 1985. Wave forces and impacts on a circular and square caisson. Coast. Eng. 2920–2932, 1984.
Van der Meer, J., d'Angremond, K., Juhl, J., 1995. Probabilistic calculations of wave forces on vertical structures. In: Proceedings of the 24th International Conference on Coastal Engineering. Kobe, Japan, pp. 1754–1767. October 23-28, 1994.
Van Doorslaer, K., De Rouck, J., Audenaert, S., Duquet, V., 2015. Crest modifications to reduce wave overtopping of non-breaking waves over a smooth dike slope. Coast. Eng. 101, 69–88.
van Gent, M., 1995. Wave Interaction with Permeable Coastal Structures. Ph.D. thesis. Civil Engineering and Geosciences, Delft University.
Vicinanza, D., Margheritini, L., Kofoed, J.P., Buccino, M., 2012. The SSG wave energy converter: performance, status and recent developments. Energies 5 (2), 193–226.
Vicinanza, D., Contestabile, P., Nørgaard, J.Q.H., Andersen, T.L., 2014. Innovative rubble mound breakwaters for overtopping wave energy conversion. Coast. Eng. 88, 154–170.
Vicinanza, D., Di Lauro, E., Contestabile, P., Gisonni, C., Lara, J.L., Losada, I.J., 2019. Review of innovative harbor breakwaters for wave-energy conversion. J. Waterw. Port Coast. Ocean Eng. ASCE 145 (4). July 2019.
Zelt, J., Skjelbreia, J.E., 1993. Estimating incident and reflected wave fields using an arbitrary number of wave gauges. In: Proceedings of the 23rd International Conference on Coastal Engineering, pp. 777–789. October 4-9, 1992, Venice, Italy.